

Impact of Municipal Water Characteristics on Corrosion of Steel and Copper Piping

By

Harsha Prasad

A Thesis Submitted to the Faculty

of the

WORCESTER POLYTECHNIC INSTITUTE

in partial fulfillment of the requirements for the

Degree of Master of Science

in

Environmental Engineering

April 2016

Approved:

Dr. Jeanine Plummer, Major Advisor

Dr. John Bergendahl, Committee Member

Abstract

This research evaluated corrosion and scale deposition in steel and copper pipe sections from apartment complexes located in Rhode Island (RI), Massachusetts (MA), and Maryland (MD). Piping samples from these locations had corroded at an accelerated rate and consisted of HVAC piping, and domestic copper pipes. Pipes were analyzed by scanning electron microscopy (SEM) and electron dispersive spectroscopy (EDS) to quantify the elemental composition of the samples. The water chemistry of each system was compared to the elemental data to determine correlations.

Particular elements from the EDS analysis in comparison to the water quality parameters, Langelier Saturation Index, and Larson Skold indices exhibited inverse and direct correlations. The deposition of corrosion product and scales occurred in all systems that had implemented corrosion control in the form of pH adjustment and inhibitors to prevent infrastructure degradation. Although measures were taken to prevent corrosion, the current practices were not effective at the current dosing rate showing that the municipalities could consider other options such as phosphate blend inhibitors and lime as effective corrosion control mechanisms.

Acknowledgements

This thesis would not have been possible without the continued support of my advisor Dr. Jeanine Plummer of the Civil and Environmental Engineering department at Worcester Polytechnic Institute. Professor Plummer has fostered a passion in this field and I thank her for her support throughout my undergraduate and graduate education. I would like to thank by undergraduate advisor Dr. John Bergendahl for being a mentor and major influence on my decision to pursue graduate studies.

I would like to thank Gregory Hendricks and Lara Strittmatter of the University of Massachusetts Medical School, Worcester, MA for allowing me to use the Core Electron Microscope Facility to complete my data analysis and their assistance throughout the data acquisition phase to guarantee the desirable results.

I would also like to acknowledge collaborator Robert Ferrari of Northeast Water Solutions Inc. for providing the samples to make this project possible and his assistance by providing necessary information to make this paper possible. I would like to thank Sarah Chamberlain of the WPI Mechanical Engineering department, Washburn Labs, for taking time out of her day to assist me in sample modification for my research goals.

Lastly, I would like to thank my family and friends for supporting me through my academic career here at WPI. This research and paper would not have been possible without their unconditional support.

Table of Contents

Abstract	i
Acknowledgements	ii
Table of Contents	iii
List of Tables	v
List of Figures	vi
1.0 Introduction	1
1.1 Causes of Corrosion	1
1.1.1 Water Chemistry	3
1.1.1.1 pH.....	3
1.1.1.2 Alkalinity	4
1.1.1.3 Total Dissolved Solids (TDS).....	4
1.1.1.4 Temperature	5
1.1.2 Flow rates.....	5
1.1.3 Summary of Water Characteristics	5
1.2 Corrosion Indices	7
1.2.1 The Langelier Saturation Index (LSI).....	8
1.2.2 Larson-Skold Index.....	10
1.3 Types of Corrosion Prevalent	11
1.3.1 Physiochemical Corrosion	12
1.3.2 Physical Corrosion	13
1.3.3 Biological Corrosion.....	14
1.3.3.1 Biofilm Formation	14
1.3.4 Bacteria	15
2.0 Methods	18
2.1 Pipe Sample Information	18
2.1.1 Pipe Data	18
2.1.2 Water Quality Data	20
2.2 SEM EDS Analysis	20
2.2.1 Sample Preparation at UMass Worcester	21
2.2.2 Sample Images	21
2.2.3 Sample Spectra.....	22
3.0 Results	24
3.1 Source Water and Corrosion Control Programs	24
3.1.1 MA	24
3.1.2 RI.....	25
3.1.3 MD	25
3.2 Average Water Quality Data	25
3.3 Corrosion Indices	26
3.4 Pipe Sample Overview	27
3.5 SEM with EDS Data Analysis	28
3.5.1 Steel Corrosion EDS Data	29
3.5.2 Copper Corrosion EDS Data.....	30
3.5.3 MA Corrosion EDS Data	32

3.5.4 RI Corrosion EDS Data	32
3.5.5 MD Corrosion EDS Data	33
3.6 Correlations between Water Quality and EDS Data	33
3.6.1 Steel Samples	34
3.6.2 Copper Samples	37
3.7 Correlations between Corrosion Indices and EDS Data	38
3.7.1 Steel Samples	38
3.7.2 Copper Samples	41
3.8 Summary of Correlations	42
4.0 Discussion	44
4.1 Analysis of Results.....	44
4.1.1 Steel and Copper Analysis	44
4.1.1.1 Steel.....	44
4.1.1.2 Copper.....	45
4.1.2 MA Analysis	45
4.1.3 RI Analysis.....	46
4.1.4 MD Analysis	46
4.2 Alternative Corrosion Control Methods	47
4.2.1 Interior Pipe Coatings	47
4.2.2 Sodium Silicate	48
4.3 Recommendations	48
4.4 Future Research into Phosphate Mechanisms.....	49
4.4.1 Application of Phosphate: Experimental Tests.....	49
4.5 Limitations of Analysis	50
References	52
Appendix A: Pipe Sample Information.....	54
Appendix B: SEM Sample Spectra Reports	59

List of Tables

Table 1: Values of A and B (Singeley 1984)	9
Table 2: LSI Value Interpretation.....	9
Table 3: Interpretation of Larson Skold Values	11
Table 4: Bacterial Classification of Anaerobic Bacteria (Beech et al. 2000).....	16
Table 5: Electron Transport Mechanism for Biological Corrosion (Kakooei et al. 2002).....	17
Table 6: Classification of Pipe Samples	19
Table 7: Average Water Quality Data	26
Table 8: Langelier and Larson Skold Index Values	26
Table 9: MA Pipe Samples.....	28
Table 10: RI Pipe Sample.....	28
Table 11: MD Pipe Samples.....	28
Table 12: Strength of Correlation Value (Stats Tutor 2016).....	34
Table 13: Steel EDS 'Face' Correlation with Water Quality	35
Table 14: Steel EDS 'Cross' Correlation with Water Quality.....	36
Table 15: Copper EDS 'Face' Correlation with Water Quality	37
Table 16: Copper EDS 'Cross' Correlation with Water Quality.....	38
Table 17: Steel EDS 'Face' Correlation with LSI and LSK.....	39
Table 18: Steel EDS 'Cross' Correlation with LSI and LSK.....	40
Table 19: Copper EDS 'Face' Correlation with LSI and LSK.....	41
Table 20: Copper EDS 'Cross' Correlation with LSI and LSK	42
Table 21: Steel and Copper Correlation Comparison.....	43
Table 22: Coatings for Pipe Walls (Singeley 1984).....	47

List of Figures

Figure 1: Annual Corrosion Cost of Utilities (Gerhardus et al. 2002)	2
Figure 2: Three Stages of the Romero Mechanism (Kakooei et al. 2002)	15
Figure 3: Steel Sample Elemental Face Composition	29
Figure 4: Steel Sample Elemental Cross-Section Composition	30
Figure 5: Copper Sample Elemental Face Composition	30
Figure 6: Copper Sample Elemental Cross-Section Composition	31
Figure 7: MA Face and Cross Elemental Composition	32
Figure 8: RI Face and Cross Elemental Composition	32
Figure 9: MD Face and Cross Elemental Composition	33

1.0 Introduction

This research assessed the impact of water chemistry on corrosion of steel and copper pipes exposed to municipal water. The systems include potable water piping from MD and RI and potable and HVAC piping from MA. The piping materials from these locations include carbon steel, galvanized steel, and copper. The pipes demonstrated various forms of corrosion as a result of water chemistry such as elevated chloride levels. The primary forms of corrosion that occur in distribution systems include chloride-induced corrosion, pitting corrosion, scale deposits, and microbially induced corrosion.

1.1 Causes of Corrosion

The purpose of studying corrosion is to help understand its causal factors due to its destructive mechanisms that have detrimental economic and engineering effects (Charng and Lansing 1982). Corrosion is a prevalent issue in the water industry due to the cost of infrastructure and the safety regulations required to prevent issues with public health (Singeley 1984). A study carried out by the National Association of Corrosion Engineers (NACE) International assessed the cost of corrosion of the five major sectors of the U.S. economy in 2002 including: infrastructure, utilities, transportation, government, and manufacturing (Gerhardus et al., 2002). The sector that was applicable to this research was the utilities, which totals to \$47.9 billion dollars annually. The distribution of the utilities can be seen in Figure 1.

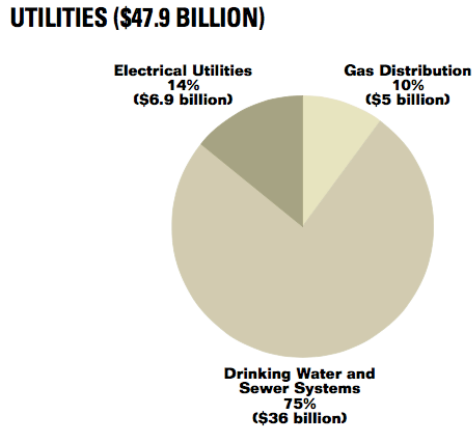


Figure 1: Annual Corrosion Cost of Utilities (Gerhardus et al. 2002)

The figure above highlights the individual components that comprise the utilities including gas distribution, electrical utilities, and drinking water and sewer systems. The drinking water and sewer systems are seventy-five percent of the total annual cost totaling \$36 billion dollars annually as of 2002 (Gerhardus et al. 2002). This value incorporates the cost of infrastructure repair, water lost from leaks, protective linings, and the use of corrosion inhibitors.

In addition to the cost of managing utilities, an important factor to consider is the risk to public health. In 1991, the EPA introduced the lead and copper rule (LCR) to regulate public exposure to these elements through drinking water due to detrimental effects to human health (Lead 2004). The treatment technique as part of the LCR involves monitoring lead and copper concentrations to identify whether lead levels exceeded 15 parts per billion (ppb) and copper exceeds 1.3 parts per million (ppm) as 90th percentile values (Lead 2004). If the values exceed the threshold, the municipality has to inform the public and take the proper precautionary measures to reduce further exposure.

The Centers for Disease Control and Prevention (CDC) recommends public health actions for lead concentrations in children exceeding 5 micrograms per deciliter. For children, the exposure to low concentrations of lead causes behavior and learning problems, slowed

growth, and anemia (Lead 2004). For pregnant women the lead can accumulate in bones along with calcium and is released into the fetus during bone formation causing reduced growth of the fetus and premature birth (Lead 2004) (CDC 2016). In adults, lead exposure can cause reproductive problems, cardiovascular effects, and decreased kidney function.

An important aspect of providing clean drinking water is the rate and extent at which the corrosion occurs, which is dependent on the pH, alkalinity, total dissolved solids (TDS), temperature, dissolved oxygen, hardness, flow rate and pipe material. Corrosivity indices can be used to quantify some of these factors.

1.1.1 Water Chemistry

In municipal water systems, the relationship between pH, alkalinity, sulfates, chlorides, total dissolved solids (TDS), and temperature are important parameters to consider when analyzing causal factors for corrosion (LeChevallier et al. 2016). Studies carried out by Pusan National University in Korea (Kim et al. 2008) and (LeChevallier et al. 2016) identified these parameters as the most important when determining scaling and corrosion potential. Manipulation of these constituents was concluded as the primary measures for corrosion control in distribution systems (Kim et al. 2008). The roles of each of these parameters in distribution systems are discussed below.

1.1.1.1 pH

Monitoring the pH is used to determine the propensity of a system to form corrosive water or potential for scale deposition in addition to other constituents. Raising the pH is used as a form of corrosion control for distribution systems. A low pH naturally occurring in the system contributes to increased carbonic acid in the system creating aggressive water that promotes and accelerates corrosion. An increase in the pH increases the overall ability of the water to create scale deposit (Leitz and Guerra 2013) by creating carbonate, CO_3^{-2} instead of bicarbonate HCO_3^- .

1.1.1.2 Alkalinity

Measurement of alkalinity is reported in units of mg/L of CaCO₃ in solution. This parameter is the ability of a water to resist changes in pH by acting as a natural buffer, and increasing the concentration contributes to more carbonate (CO₃⁻²) and bicarbonate (HCO₃⁻) in the water (LeChevallier et al. 2016). For water that is aggressive with a low pH, increasing the pH will convert carbonic acid to bicarbonate (HCO₃⁻) ions seen in Reaction 1. In contrast a decrease in pH will convert the bicarbonate in solution to carbonic acid, seen in Reaction 2. In both cases, increasing the alkalinity will increase the total concentration of carbonate species in the water system.



Monitoring of alkalinity in correlation with pH is used to identify the propensity of a system to experience scaling by evaluating concentrations of bicarbonate and carbonate ions since calcium carbonate precipitates at high pH values.

1.1.1.3 Total Dissolved Solids (TDS)

Another factor that causes increased corrosion rates is high dissolved solids in solution. The constituents that contribute to this parameter include minerals, salts, metals, cations or anions dissolved in water. The salts included elements such as calcium, magnesium, potassium, sodium, iron, and chlorides. Measurement of the overall TDS incorporates the hardness, which consists of the calcium and magnesium concentrations as well as other multivalent cations. Increased levels of chlorides and sulfates contribute to accelerated corrosion in iron, copper and galvanized steel piping (Singeley et al. 1984) by reacting with the metallic surface while the sulfates correlate to bacterial formations (Kakooei et al. 2012, LeChevallier et al. 2016). The presence of other

elements such as silicates and phosphates has the potential for inhibiting corrosion and forming protective films. The addition of these constituents in the system can also be responsible for inducing chemical or bio-chemical corrosion.

1.1.1.4 Temperature

The temperature of water has varied effects on corrosion and is directly related to other parameters such as dissolved oxygen (DO). Warmer water has a lower DO saturation concentration than colder water, which has a higher DO concentration. The warmer water has increased biological rate of growth in the form of microbially induced corrosion (MIC) and is affected by electro-chemical corrosion due to less oxygen and electrons in the system.

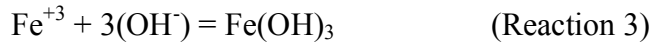
1.1.2 Flow rates

Increasing the flow rate creates turbulent flow that leads to degradation of the interior diameter of the pipe in addition to erosion corrosion if there are high TDS concentrations (Geiger and Esmacher 2012). In addition to turbulent flow, a high velocity water increases the rate at which dissolved oxygen interacts with metal surfaces, creating a much more rapid oxidation of the material. In contrast, lower velocity water causes stagnation in a system that can enable chlorides to react with the pipe interface leading to different forms of corrosion including chloride-induced corrosion.

1.1.3 Summary of Water Characteristics

Varying combinations of the parameters listed above are responsible for different forms of corrosion in distribution systems. For a low pH and low alkalinity system, the resulting corrosion is typically comprised of uniform pitting and pinhole corrosion on the interior diameter of the pipe (Lahlou 2003) due to the acidity of the water and its aggressive nature (Oliphant 2010). In contrast, a higher alkalinity decreases the acidity of a system but can cause precipitation of free

ions in solution such as calcium, iron, and magnesium in the form of scale deposits. For example, ferrous iron precipitates to ferric oxides as shown in Reaction 3.



The available hydroxide ions are able to reduce the iron making it ferric and non-soluble. If the water chemistry has elevated TDS and alkalinity, the layer of scale deposit that forms acts as a barrier on the inside of the pipe to prevent degradation of the pipe material. Mechanisms analyzed by the Technical Institute in Lisbon, Portugal concluded that the formation of ferric oxides and ferric chlorides occurred as a result of the chloride displacing the oxygen on the inside diameter of the pipes to form deposits (Montemor et al. 2003). Another mechanism stated the decreased oxygen vacancies enabled the chloride to react with the inner diameter of the pipe causing different methods of corrosion to occur such as pitting and crevice corrosion that led to pipe material leaching (Montemor et al. 2003). Due to different forms of corrosion that occur such as pitting and crevice corrosion, an anoxic zone between the interior of the pipe and scale deposit was a suitable environment for the formation of corrosion-causing bacteria such as sulfate or iron bacteria (Lahlou 2003, Charng and Lansing 1982). In some cases, there have been higher biofilm densities in systems that consist of ferrous materials in the presence of disinfectants (Abernathy 2006).

Although chlorine is often introduced to kill the microorganisms (Lahlou 2003), the effects of chloride-induced corrosion and deposition of ferric oxides and ferric chlorides can create the ideal environment for microbially induced corrosion (Chawla et al. 2012) under the precipitates that form (Javaherdashti 2008). Elevated levels of sulfates and free iron in the water contribute to the formation of iron reducing bacteria (IRB) and sulfur reducing bacteria (SRB)

based on research conducted by the Center for Corrosion Research in Malaysia (Kakooei et al. 2012). The main parameters that contribute to steel degradation include the presence of electrons from electrochemical potential corrosion. The availability of electrons can arise from multiple sources including the presence of dissolved oxygen (Kakooei et al. 2012). A study carried out by the Oliphant (2010) analyzed the primary forms of corrosion for copper-piping systems based on the water quality parameters of interest. The main causes of failure occurred due to a high pH, low concentration of bicarbonate, and microbial growth as a result of sulfur reducing bacteria due to stagnated water. In addition to those parameters, the presence of elevated chloride concentrations in the system were detrimental by reacting with the internal diameter of the pipe and releasing oxygen from the passive layer (Montemor et al. 2003) providing more electrons for chemical potentials to form.

1.2 Corrosion Indices

To quantify the formation of scaling and susceptibility to corrosion within piping systems, indices have been developed to determine the propensity of precipitation and corrosion of varying compounds (Leitz and Guerra 2013). The indices used to determine the probability of corrosion and scale deposition include the Langelier Saturation Index (LSI), Larson-Skold Index (LSK), Ryznar Index, and the Stiff and Davis Stability Index (S&DI) (Leitz and Guerra 2013). The S&DI index is used for water chemistry with TDS over 10,000 mg/L. The water quality data for the systems analyzed do not have TDS values in this range so this method was not used. The Ryznar index incorporates the LSI index in the calculations making this index redundant. For the purpose of this study, the LSI index and Larson Skold Index are the primary indices to identify system susceptibility to corrosion. The LSI calculation assesses the propensity for calcium carbonate precipitation in waters that have TDS below 10,000 mg/L by using the calcium,

alkalinity, and TDS concentrations. The Larson-Skold calculation incorporates the carbonate, bicarbonate, chloride, and sulfate concentrations to determine the probability of corrosion in steel piping systems. Some of the factors that should be considered when interpreting these values include temperature, kinetics of reaction, and the time required for precipitates to form as a result of kinetics (Leitz and Guerra 2013). The following sections explain the calculations and analysis of the quantitative values for the indices.

1.2.1 The Langelier Saturation Index (LSI)

The LSI is a measure of precipitation and is a function of the saturation pH and the calcium carbonate concentration present. The LSI calculation can be done with two different methods with both incorporating the difference between the saturation pH or pH_s and the actual pH of the water. The first method is calculated based on three parameters that include the negative logarithm concentration of the alkalinity and calcium, and the value C that is based on the TDS. The second method uses constants to quantify the TDS and temperature value. The calculation for the first method is below. The first two equations solve for the values needed for saturation pH, and Equations 3 and 4 solves for the LSI value (Leitz and Guerra 2013).

Equation 1, C as a function of TDS and Temperature: $C(TDS,T) = 3.26e^{-.005*T} - 0.0116 \log_{10}(TDS^3) + 0.0905 \log_{10}(TDS^2) - 0.133 \log_{10}(TDS) - 0.02$

Equation 2, Negative Logarithms of Calcium and Alkalinity:

$-\text{Log}_{10}(\text{Ca}) = \text{pCa}$
 $-\text{Log}_{10}(\text{Alk}) = \text{pAlk}$

Equation 3, Solving for saturation pH:

$pH_s = \text{pCa} + \text{pAlk} + C$

Equation 4, LSI Value:

$\text{LSI} = \text{pH} - \text{pH}_s$

The second method for calculating the LSI is the same as Equation 4 but using a different method for solving the pH_s . To incorporate the variance in temperature and TDS of the water, the constants ‘A’ and ‘B’ are used for each parameter respectively. Equation 5 below shows the calculation for this method including the concentrations from equation 2, and values for ‘A’ and ‘B’ as shown in Table 1.

Equation 5 LSI value with A and B:

$$pH_s = A + B + pCa + pAlk$$

Table 1: Values of A and B (Singeley 1984)

Water Temp Fahrenheit	Constant A	TDS (mg/L)	Constant B
32	2.6	0	9.7
39.2	2.5	100	9.77
46.4	2.4	200	9.83
53.6	2.3	400	9.86
60.8	2.2	800	9.89
68	2.1	1000	9.9
77	2.0		
86	1.9		
104	1.7		
122	1.55		
140	1.4		
158	1.25		
176	1.12		

The two different LSI calculations can yield similar answers and enables the user to find the propensity for scale with varying water quality data. Table 2 below highlights the meaning of the LSI value generated (Leitz and Guerra 2013).

Table 2: LSI Value Interpretation

LSI Index Value	Analysis
LSI < 0	Under saturated water; no scaling potential, corrosion potential due to no CaCO ₃ protective layer on interior diameter of pipes
LSI > 0	Over saturated water; high scaling potential, protective layer formed by CaCO ₃ on interior diameter of pipes
LSI = 0	Neutral water, no tendency in either direction

Although this index can determine the probability of scale deposition there are some drawbacks depending on other water quality parameters. Bench and pilot scale studies carried out by Montana State University used the Langelier saturation index as a means to quantify the CaCO_3 scale potential in their systems. The study concluded that this was a fair representation of the scale formations; however, if there are elevated sulfate concentrations the formation of CaSO_4 can give similar LSI values by substituting the calcium value from CaSO_4 for CaCO_3 (Abernathy 2006). In addition to sulfates, water with low alkalinity can't be supersaturated with CaCO_3 making the calculation ineffective regardless of the pH concentration (Abernathy 2006).

McDougall et al. (2003) utilized the LSI method for tap water from two treatment plants ('B' and 'C') with copper piping suffering from pitting corrosion. The source water had a pH of 7.7, elevated chlorides, and elevated TDS. Plant 'B' had a water temperature of 81°F and plant 'C' had a temperature of 61°F. The LSI values were -2.8, and -2.6 respectively showing that no scale was forming within the system (McDougall et al. 2003). Since no protective scale was present on the interior diameter of the pipe, the chlorides were able to react with the interior diameter causing corrosion (McDougall et al. 2003, Montemor et al. 2003, Abernathy 2006).

1.2.2 Larson-Skold Index

The benefit of the Larson-Skold index in comparison with the LSI is the inclusion of chlorides and sulfate ions with respect to the concentrations of carbonate and bicarbonate ions (Leitz and Guerra 2013). The chlorides are responsible for chloride-induced corrosion and the sulfates are a precursor to sulfur reducing bacteria. This index was developed for steel piping which is a primary material used for the systems analyzed in this study. The formula used to quantify the relationship between carbonate, bicarbonate, chlorides and sulfates can be seen below in

Equation 6. The concentrations for each of the parameters are converted to equivalents per liter (Leitz and Guerra 2013).

Equation 6 Larson Skold Calculation:

$$L\&SkI = \frac{(Cl^- + SO_4^{-2})}{(CO_3^{-2} + HCO_3^-)}$$

Table 3: Interpretation of Larson Skold Values

Larson Skold Index Value	Analysis
L&SkI < 0.8	Chloride and Sulfate are negligible
0.8 < L&SkI < 1.2	Chloride and Sulfate may interfere with inner diameter of pipe and interact with formation of protective coatings
L&SkI > 1.2	High Corrosion rates expected

The use of this index is applicable to steel piping for distribution systems, and provides insight of the long term effects of elevated chlorides and sulfates (Abernathy 2006). A study by the LeChevallier et al. (2016) assessed the disinfection efficiency on biofilms by utilizing the Larson-Skold index to identify changes in the water chemistry over time. The study revealed that the current treatment practices caused the calculation to vary due to the addition of alum, ferric salts, and chlorine. As a result the pH of the water decreased, causing a decrease in the alkalinity levels, therefore increasing the LSK value. In contrast, the use of lime, soda ash, and sodium bicarbonate increased the alkalinity thereby reducing the LSK value (LeChevallier et al. 2016). Due to seasonal changes, the LSK value fluctuated between 1 to 30, with the high values occurring when the alkalinity was below 10 mg/L CaCO₃ (LeChevallier et al. 2016). This index does not incorporate the concentration of CaCO₃ and its precipitation which can affect the overall corrosivity of the water.

1.3 Types of Corrosion Prevalent

The two main types of corrosion include physiochemical and biological corrosion.

Physiochemical corrosion includes seven main categories including: galvanic, concentrated cell,

dezincification, pitting, inter-granular, stress, and erosion impingement cavitation. The biological corrosion is caused by iron reducing bacteria (IRB), nitrifying bacteria, and sulfur reducing bacteria (SRB) in water systems. The following sections highlight the main types of corrosion in each category and their overall effect in distribution systems.

1.3.1 Physiochemical Corrosion

The occurrence of physiochemical corrosion occurs as a singularity and in conjunction with other types of corrosion. For distribution systems that have varying materials, a point of contact where corrosion is likely to occur is a pipe joint between two different alloys that creates an electrochemical potential (Geiger and Esmacher 2012). This potential refers to the flow of electrons from an anode and cathode between the corrosion sites. This electron flow is a site of chemical activity that makes it a major contributor to internal corrosion of water distribution systems. Regions where electrochemical potentials form include pipe sections where stress cracks occur as well. A driving force for electron flow and chemical potential arises from oxygen in the system (Charng and Lansing 1982) and plays a role in what type of corrosion will be prevalent.

An example of electrochemical corrosion is galvanic corrosion and concentrated cell corrosion. This occurs as a result of galvanized steel when in contact with another material such as copper (Singeley et al. 1984). Factors that affect galvanic corrosion include the distance between the cathode and anode on the inner diameter of the pipes and surface area of the material. Concentrated cell corrosion also requires a chemical potential from varying materials but relies on oxygen as the limiting factor and is typically associated with crevice corrosion such as cracks within the pipe interior.

Dezincification occurs as a result of high zinc concentrations in the water and contributes to pipe degradation by both covering pits and crevices creating an anoxic environment or

creating a film on the interior diameter of the pipe. The zinc deposition is recognized by red pigments and has a higher propensity to occur in brass structures. The reduction of this process is possible with the addition of arsenic, antimony, or phosphorous to the alloy itself (Charng and Lansing 1982).

1.3.2 Physical Corrosion

Depending on the flow rate of the system, different types of corrosion occur as a result such as pitting corrosion, erosion impingement cavitation, and stress corrosion. Pitting corrosion is primarily linked with stagnant aqueous solution, and develops on horizontal steel surfaces and corrodes into the material (Oliphant 2010, Geiger and Esmacher 2012). Pitting occurs in small patches and varies in frequency of occurrence, size, and depth into the material (Charng and Lansing 1982) and occurs in copper plumbing systems that do not exceed 40° Celsius with a pH between 7 and 8 (Oliphant 2010). The passive layer of the interior diameter of the pipe is penetrated by aggressive anions like chlorides or bromide and reacts with the pipe wall (Kritzer 2004, LeChevallier et al. 2016). If there is an increase in temperature and conductivity, or decrease in flow rate, the rate of corrosion will increase.

Erosion impingement cavitation is caused by the abrasion of the pipe material from the flow of a fluid or gas and occurs in three stages: the erosion of the interior diameter, impingement of the material, and cavitation. All three stages are affected by the aeration and release of gas particles and an increase in TDS. Water with high TDS with large particles that are coarse and rough creates directional grooves and gouges on the interior diameter of the pipes (Charng and Lansing 1982) as part of the erosion and impingement. Impingement is associated with turbulent flow of a liquid that causes corrosion from pure force. Cavitation occurs as a result of voids or vacuums and has been found near the propeller after a pump and happens as a

result of a collapsing vacuum bubble, which releases energy in an explosive effect damaging the pipe material (Charng and Lansing 1982).

Stress corrosion is attributed to exterior forces on the pipe that cause physical changes to the material (Geiger and Esmacher 2012). Internal stressors include non-uniform deformation during cold working, or from high temperature fluctuations within in the material (Charng and Lansing 1982). In addition to temperature, fixtures within the pipe such as rivets, bolts, and various shrink fits are prone to be affected by pressure differentials. A combination of high stress and electrochemical reactions within the pipe accelerate the rate of corrosion.

1.3.3 Biological Corrosion

The formation of biofilms within piping system contributes to the formation and viability of microorganisms existing such as bacterial colonies of sulfur reducing bacteria (SRB), iron reducing bacteria (IRB) and nitrogen fixing bacteria.

1.3.3.1 Biofilm Formation

Biofilms play a key role in the formation of corrosion within piping systems. The formation is dependent on the aqueous environment where the metal is immersed. The first stage of biofilm formation is the creation of the conditioning film (Javaherdashti 2008). This is formed by the electrostatic arrangement of a wide variety of proteins and organic compounds that are reacting with the water chemistry. At this point, sessile bacteria that are stationary attach to the conditioning film. After the biofilm is formed the outer cells of the film have access to a more nutrient rich environment and will start utilizing this resource at a faster rate than the cells that are deeper within the biofilm creating a difference in growth rates. As a result of this cell formation, the outer cells increase in population and the film acts as a bio net to trap floating organic and inorganic particles that are floating within the solution (Javaherdashti 2008) making

the biofilm even thicker. In Figure 2 a proposed mechanism for biofilm formation is seen in addition to the type of corrosion that occurs as a result of sulfur reducing bacteria.

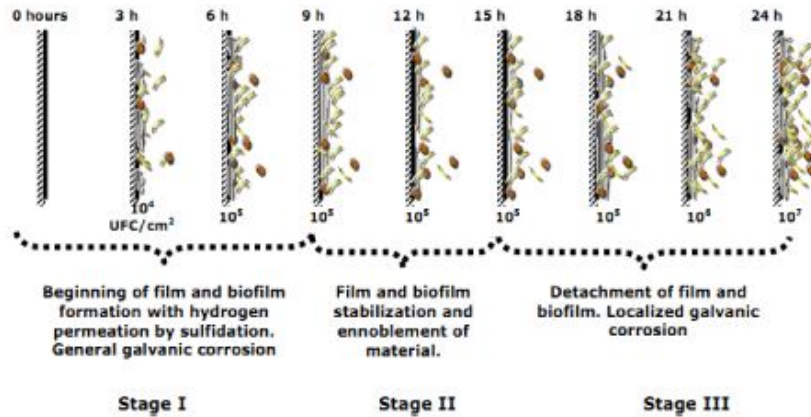


Figure 2: Three Stages of the Romero Mechanism (Kakooei et al. 2002)

The resulting biofilm layer provides the medium for bacteria to corrode the interior diameter of the pipe. The mechanism above incorporates the electron availability from galvanic corrosion and the formation of the film within the cathode and anode ends of the pipe (Kakooei et al. 2002), showing that multiple types of corrosion can occur simultaneously.

Another theory suggests that the formation of exopolysaccharidic substances (EPS) help the fragile bacteria in the biofilm survive from external factors that are life threatening to the bacteria such as the presence of chlorine. In addition to survival, the EPS has been shown to increase their capacity to absorb more food by expanding their surface area (Javaherdashti 2008).

1.3.4 Bacteria

The bacteria that are responsible for corrosion include aerobic and anaerobic bacteria. The primary aerobic bacteria are *E. coli* that function from oxygen respiration (Beech et al. 2000). The main groups of bacteria are grouped based on the constituents responsible for growth that include sulfur reducing bacteria, nitrifying bacteria, ferrous iron conversion, and carbonate

respiration. For the purpose of this study the most relevant anaerobic bacteria are sulfur-reducing bacteria (SRB).

Table 4: Bacterial Classification of Anaerobic Bacteria (Beech et al. 2000)

Electron Acceptor	Product	Respiration/ <i>Organism Example</i>
NO_3^- , NH_3	NO_2^- , N_2O , N_2 , NH_4^+	Nitrate respiration, denitrification process; <i>Pseudomonas stutzeri</i>
S^{-2}	SO_4^{-2}	Sulfate respiration, numerous bacteria responsible; <i>Desulfovibrio</i>
S	S^{-2}	Sulfur respiration, facultative anaerobic bacteria; <i>Desulfuromonas acetoxidans</i>
CO_2	Acetate, Methane	Carbonate respiration for both bacteria Acetogenic bacteria: <i>Clostridium aceticum</i> Methanogenic bacteria: <i>Methanobacterium</i>
Fe^{+3}	Fe^{+2}	Iron respiration, <i>Alteromonas putrefaciens</i>

Sulfur reducing bacteria fix sulfur from two different sources and produce hydrogen sulfide, sulfur, and sulfates as a byproduct (Kakooei et al. 2002, Beech et al. 2000), Nitrifying bacteria fix ammonia and nitrate and produce nitric acid, nitrate, nitrogen, and nitrous oxide. Iron fixing bacteria can convert ferrous iron from soluble ferrous salts into insoluble ferrous oxide (Charnig and Lansing 1982) since $\text{Fe}^{+3}/\text{Fe}^{+2}$ can react with hydroxide as previously shown in Reaction 3.

The bacterial group of interest is SRB since the water quality of the three locations includes sulfates. The formation of biofilms within the distribution systems enables the bacteria to thrive if there are nutrients and sulfur available and can be enhanced by other types of corrosion such as stress corrosion that leads to failure of the material. As identified in Figure 2, the presence of electrochemical conditions benefits SRB formation by cathode and anode depolarization of the metal surface.

The most recent mechanism incorporates the Romero mechanism in Figure 2 with the Bio-catalytic Cathodic Sulfate Reduction (BCSR) as of 2009 (Kakooei et al. 2002). This

involves the sulfate reduction at the cathode end by protein clusters consuming the electrons released by iron dissolution at the anode end with ferredoxin. The electron transport occurs with the help of a biocatalyst and the interface of biofilm formation (Kakooei et al. 2002). The total reaction from Table 5 summarizes the two reactions that occur in the cathodic and anodic terminals that are responsible for biological corrosion (Kakooei et al. 2002).

Table 5: Electron Transport Mechanism for Biological Corrosion (Kakooei et al. 2002)

Potential	Chemical Formula	Term Clarification
Anode	$4\text{Fe} - 6\text{-Fe}^{+2} + 8\text{e}^{-}$	The '6' represents a protein cluster formation of Iron that is responsible for electron transport in the anodic end to the cathodic end, known as a ferredoxin
Cathode	$\text{SO}_4^{-2} + 8\text{H}^{+} + 8\text{e}^{-} - 6\text{-HS}^{-} + \text{OH}^{-} + 3\text{H}_2\text{O}$	The '6' represents a protein cluster formation of hydrogen sulfide with free electrons, responsible for the 8e^{-} acceptance from the cathodic end
Total	$4\text{Fe} + \text{SO}_4^{-2} + 3\text{Fe}(\text{OH})_2 (\text{s}) + 2\text{OH}^{-} + 4\text{H}_2\text{O} \text{ } 6\text{FeS} (\text{aq})$	Resulting terms are solid ferric hydroxide and aqueous cluster of ferrous sulfide, with free iron, sulfates, and hydroxide

2.0 Methods

The main objective of this study was to analyze piping sections from various water systems from Massachusetts (MA), Rhode Island (RI), and Maryland (MD) in order to identify scale deposit and corrosion product. The anonymity of the particular locations is preserved by not identifying the exact municipality. The interior diameter of the pipes was examined to determine elements present by using a material science approach. The method chosen to fulfill this objective was Scanning Electron Microscopy (SEM) and electron dispersive spectroscopy (EDS). The elemental composition of the pipe interiors was compared to water quality data for each system to determine correlations.

2.1 Pipe Sample Information

The pipe sections were attained from Northeast Water Solutions Inc., Exeter, RI and consisted of copper pipe sections that had diameters ranging from one-half inch to two inches with lengths ranging from one to two feet. The galvanized and carbon steel pipes had diameters ranging from two to six inches with lengths between five inches to three feet.

2.1.1 Pipe Data

The following section summarizes the pipe sections from the MA, RI, and MD municipalities that were analyzed for this study shown in Table 6.

Table 6: Classification of Pipe Samples

Sample ID	Material	Composition	Supply	System	Temp.	Loop
2	Galvanized Steel	Pipe	MA	Dry Sprinkler	Cold	Open
3	Galvanized Steel	Well Pipe	RI	Potable	Cold	Open
4	Carbon Steel	Pipe	MA	Wet Sprinkler	Cold	Open
5	Carbon Steel	Pipe	MA	HVAC	Hot	Closed
6	Carbon Steel	Manifold Pipe	MA	HVAC	Hot	Closed
7	Copper	Pipe	MD	Potable	Cold	Open
8	Carbon Steel	Spool	MA	HVAC	Warm	Closed
9	Carbon Steel	Spool	MA	HVAC	Warm	Closed
10.1	Copper	Pipe	MD	Potable	Cold	Open
10.4	Carbon Steel	Pipe	MD	Potable	Hot/Cold	Open
10.5	Carbon Steel	Elbow Fitting	MD	Potable	Hot/Cold	Open
10.6	Copper	Pipe	MD	Potable	Hot/Cold	Open
10.7	Copper	Pipe	MD	Potable	Cold	Open
10.8	Copper	Pipe	MD	Potable	Hot/Cold	Open
11.1	Carbon Steel	Pipe	MA	HVAC	Hot	Open
11.2	Carbon Steel	Pipe	MA	HVAC	Hot	Open
11.4	Carbon Steel	Pipe	MA	HVAC	Hot	Open
11.5	Carbon Steel	Pipe	MA	HVAC	Hot	Open
11.8	Carbon Steel	Pipe	MA	HVAC	Hot	Open
12.1	Copper	Valve	MA	Potable	Hot/Cold	Open

The pipe sections consist of HVAC piping, sprinkler systems, and potable water piping. All samples are from apartment complexes, none of which are commercial. The dry sprinkler indicates a system that does not normally have water in it, but can have water vapor condensation and the wet sprinkler identifies a sprinkler system with water. Some of the HVAC pipes were labeled as spools while the other pipes are part of the main heating pipe system. Some of the pipes exhibited water vapor condensation corrosion on the exterior as a result of insulation. Depending on the size of the sample, some pipe sections were cut through the diameter of the pipe with a band saw. The resulting sample piece was a ring one inch in thickness to make them more manageable. After cutting the samples, the cross sections were stored in a dry environment to prevent any further oxidation of the sample material. In order to

process these samples without bias, they were numbered and the data on the pipe characteristics were not revealed until after the SEM elemental analysis was completed. This was done to keep consistency during sampling and data processing.

2.1.2 Water Quality Data

The water quality data for each municipality was compiled for this study. The variables of interest for these systems include pH, alkalinity, TDS, chloride, sulfate, and calcium. The data from MD was taken from five years of data from the municipality water quality reports from January 2010 to 2014 from the website for tap water quality. The data from MA was obtained from the water department and consisted of once per month samples over a three-year period of data from 2013-2015. The water quality information for RI was comprised of data from 2008/2009 from Northeast Water Solutions Inc. (NWSI).

2.2 SEM EDS Analysis

The elemental compositions within each the sample were determined by scanning electron microscopy (SEM). In addition to generating SEM images at 1000X magnification, the use of electron dispersive spectroscopy (EDS) software was run on each image to yield the elemental compositions in weight percent on the sample interface. The SEM used was an Oxford Instruments FEI Quanta 200, which utilized EDS software INCA 350. Oxford Instruments from Concord, MA manufactured the SEM used for the data acquisition. The instrument was housed at the University of Massachusetts Medical School, Core Electron Microscopy Facility, Worcester, MA.

The instrument had an overall sample run time of twenty to thirty minutes including EDS analysis. A copper corrosion study done by Burleigh et al. (2014) analyzed their piping sections with SEM and EDS software to identify the corrosion deposits on the interior diameter of the

pipes and the pits that formed. This method is a practical and appropriate method to analyze the elemental layering and deposition.

2.2.1 Sample Preparation at UMass Worcester

The SEM required minimal preparation for sample analysis. Using the ring section from the main pipe, quarter inch samples were cut from the cross sections with a dremel to find the best sample to represent the pipe section. The best sample piece was chosen based on observable corrosion product on the interior diameter. After the cutting process, the sample was taped down to an interchangeable stage with copper tape to ground the sample and then carbon tape to support the sample on the stage to prevent it from falling, after it was loaded into the microscope. Two profiles of the sample were used for this study: (1) A plan or face image of the interior diameter of the pipe surface and (2) a cross-section of the pipe from the outer diameter to the inner diameter that was in contact with the water.

2.2.2 Sample Images

Before placing the sample on the stage, the vacuum chamber was vented which took roughly one minute. When the vacuum pressure normalized, the sample was loaded onto the stage and screwed in place with a grommet and screwdriver. After closing the door to the chamber, it was then pumped to create a vacuum. When the vacuum reached its appropriate threshold, a green icon indicated that the electron beam could be turned on. Once the beam was turned on, the sample could be seen on the computer screen linked to the microscope. The face view was analyzed first, and then the sample was removed and rotated 90° to analyze the cross sectional view. After the sample was loaded, the magnification, contrast, and focus were set. The magnification was set to 1000X at a voltage of 30kV to be consistent.

The control board was used in conjunction with three images developed as the magnification increased. The images developed consisted of secondary electron image (SEI),

backscattered electron image (BSI), and mixed image that differed due to the electrons received by the detector. The use of the SEI and BSI images in tandem was used to focus the image better to try and attain the best image possible of the corrosive deposits. The mixed image overlaid the SEI and BSI images and highlighted changes in layers as magnification increased. The scan time for these images to be generated took 30 microseconds and could be adjusted depending on the resolution in order to identify specific layers of interest and focus the image. The images generated were then used for the EDS software analysis.

2.2.3 Sample Spectra

After developing these images, the SEI image was uploaded to the INCA software, which enabled the user to select different locations on the sample to attain an elemental spectrum. The points of interest for each sample consisted of three to four locations on the sample face as follows:

Face Image

- Face 1: Estimate of Surface of Corrosion
- Face 2: Mid-Level Sample Point
- Face 3: Surface of Corrosion and Pipe Interior
- Face 4: Estimate of Pipe Interior

The points of interest for the cross-section image of the sample had three spectra points.

Cross-Section Image

- Cross I: Corrosion Deposit/Water Interface
- Cross M: Pipe/Corrosion Deposit
- Cross P: Pipe Itself

Since the actual layers could not be clearly differentiated, the spectra points required a qualitative estimation. With the main points selected, spectra were created at each desired location from the SEI image. The sample run time for each spectrum was less than two minutes and created a spectrum with various peaks identifying elemental composition found on the chosen location on the SEI image. After all the spectra were gathered, a compared image could be generated with all of the spectra to compare and contrast different concentrations from location to location. The elemental analysis for all spectra generated provided a quantitative weight percent for each element found. All of these spectra were saved on the software and compiled into a report showing the image and the respective elemental concentrations.

3.0 Results

This chapter focuses on the factors that influence corrosion in the samples analyzed. This includes the source water and corrosion control measures that were implemented to preserve the infrastructure, water quality data, the LSI and Larson Skold values calculated, and the SEM EDS data from the respective locations. Using these parameters, correlation analyses were used to compare the formation of corrosive constituents and the factors that influence corrosivity.

3.1 Source Water and Corrosion Control Programs

The three locations of study, MA, RI, and MD all have different source water origins with varying water quality parameters. To fully assess the SEM data, the source water chemistry was researched. Data on the water quality are provided in the following sections.

3.1.1 MA

The drinking water supply system for the site in MA consists of two points of collection that consist of the two reservoirs that are then stored at a collection point. The raw water is treated at a water treatment plant with processes consisting of aeration, pretreatment oxidation, coagulation and flocculation, dissolved air flotation, and then settling to remove large aggregates. The water is then treated with ozone, granulated activated carbon, and then chlorination where it is pumped to two covered storage tanks. At this point, the water pH of the water is adjusted for corrosion control, chloramines are added to provide disinfectant residual, and fluoride is added for dental health before distribution to the consumers.

To maintain drinking water standards that meet the LCR, the water department adjusts the pH to approximately 9 with a 50% solution of sodium hydroxide, at a concentration of 14 mg/L. The target pH for distribution is 9.1, and with the source water chemistry of the system, the lead and copper levels are below the actions levels of 15 ppb and 1.3 ppm respectively.

3.1.2 RI

The aquifer that supplies the system in RI is a surficial aquifer, meaning it is a shallow aquifer typically less than fifty feet in depth. For this particular aquifer the saturated thickness is estimated to be 10 feet or greater. The treatment plant processes consist of aeration and enhanced oxidation, then membrane filtration, and lastly disinfection and corrosion control measures before supplying the water to consumers. To prevent corrosion within the system, the municipality uses lime and potassium hydroxide prior to distribution for pH adjustment.

3.1.3 MD

For Maryland, a river source is used as supply where it is treated at a water treatment plant. The plant doses permanganate, powdered activated carbon, and coagulant as part of coagulation and flocculation, uses sedimentation to remove large aggregates, and does chlorine before filtration. After filtration, Ultraviolet (UV) light disinfection is used to inactivate microbes, with fluoride and chlorine added to the water. At this stage in the process, corrosion control measures consisting of lime and orthophosphate are introduced before the finished water is stored. After the water is stored, it is then pumped to the distribution system for public consumption.

3.2 Average Water Quality Data

The water quality data for the three water systems are shown in Table 7, including: pH, calcium, alkalinity, TDS, chloride, and sulfate. For Maryland, the water quality report did not provide a TDS value. Instead the conductivity was converted by multiplying the conductivity value by the constant 0.65 (Rosemount 2012). These parameters were used to calculate the Langelier and Larson Skold values.

Table 7: Average Water Quality Data

Supply	pH	Calcium (mg/L)	Alkalinity (mg/L as CaCO₃)	TDS (mg/L)	Chloride (mg/L)	Sulfate (mg/L)
MA	9.04	22.26	36.11	394.39	159.90	25.13
RI	6.60	5.50	9.80	47.40	4.33	4.20
MD	7.40	36.30	80.60	247.13	44.52	38.14

3.3 Corrosion Indices

Table 8 below shows the calculated LSI for both methods, with LSIA using Equation 3 and 4 with calcium, alkalinity, and a value for ‘C’ based on TDS, and LSIB using Equation 4 and 5 with calcium, alkalinity, and values for ‘A’ and ‘B’ based on the temperature and TDS for three different temperature values. The Larson-Skold value was calculated using Equation 6 that is independent of temperature. The pipes for MA and MD were used for both hot and cold water so LSI values were calculated at 50°F, 110°F, and 130°F. The pipes from RI were only exposed to cold water so the values were calculated at 50°F.

Table 8: Langelier and Larson Skold Index Values

Location	Temperature (°F)	LSIA	LSIB	LSK
MA	50	0.01	0.14	6.98
	110	0.68	0.75	
	130	0.84	0.95	
RI	50	-3.61	-3.34	1.07
MD	50	-1.08	-0.92	1.27
	110	-0.41	-0.31	
	130	-0.24	-0.1	

From Table 2, an LSI value below ‘0’ identifies no scaling potential and the potential for corrosion, and over ‘0’ signifies scale formation which can protect the pipe surface from

corrosion. From Table 3, a Larson Skold value below 0.8 shows no corrosion occurring, and a value between 0.8 and 1.2 indicates that chloride and sulfates may interfere with the formation of protective scale on the interior of the pipe. Any value above 1.2 indicates that there is a very high propensity for corrosion to occur.

The LSI values for MA illustrated that some scale deposition will occur in the system, while the values for RI and MD show no precipitate forming in the pipes. The lack of protective scale on the pipe can indicate the potential for water constituents to react with the interior of the pipe causing corrosion. The Larson Skold value for RI and MD are in the median category that indicates minimal interactions with the pipe material. The MA value is roughly six times greater than the index value of 1.2, and indicates that high corrosion rates will occur based on the water quality. While the LSI and Larson Skold index values for MD are in reasonable agreement with (minor to moderate corrosion), the index values for the other two sites are contradictory. In MA, the LSI values show a protective scale being formed while the Larson Skold indicates severe corrosion. In RI, the LSI indicates severe corrosion while the Larson Skold indicates only moderate corrosion.

3.4 Pipe Sample Overview

The following section summarizes all of the pipe samples and their respective locations.

Table 9: MA Pipe Samples

Sample ID	Material	Composition	System	Temp.	Loop
2	Galvanized Steel	Pipe	Dry Sprinkler	Cold	Open
4	Carbon Steel	Pipe	Wet Sprinkler	Cold	Open
5	Carbon Steel	Pipe	HVAC	Hot	Closed
6	Carbon Steel	Manifold Pipe	HVAC	Hot	Closed
8	Carbon Steel	Spool	HVAC	Warm	Closed
9	Carbon Steel	Spool	HVAC	Warm	Closed
11.1	Carbon Steel	Pipe	HVAC	Hot	Open
11.2	Carbon Steel	Pipe	HVAC	Hot	Open
11.4	Carbon Steel	Pipe	HVAC	Hot	Open
11.5	Carbon Steel	Pipe	HVAC	Hot	Open
11.8	Carbon Steel	Pipe	HVAC	Hot	Open
12.1	Copper	Valve	Potable	Hot/Cold	Open

Table 10: RI Pipe Sample

Sample ID	Material	Composition	System	Temp.	Loop
3	Galvanized Steel	Well Pipe	Potable	Cold	Open

Table 11: MD Pipe Samples

Sample ID	Material	Composition	System	Temp.	Loop
7	Copper	Pipe	Potable	Cold	Open
10.1	Copper	Pipe	Potable	Cold	Open
10.4	Carbon Steel	Pipe	Potable	Hot/Cold	Open
10.5	Carbon Steel	Elbow Fitting	Potable	Hot/Cold	Open
10.6	Copper	Pipe	Potable	Hot/Cold	Open
10.7	Copper	Pipe	Potable	Cold	Open
10.8	Copper	Pipe	Potable	Hot/Cold	Open

3.5 SEM with EDS Data Analysis

The following figures illustrate the elemental composition for the steel and copper piping samples in addition to the element values for the locations analyzed. The ‘Face’ spectra points labeled as ‘Face 1’, ‘Face 2’, ‘Face 3’, ‘Face 4’ and the ‘Cross’ spectra points labeled as ‘Cross

I', 'Cross M', and 'Cross P'. For each location, elemental values were averaged for each element. Elements that had average weight percentages less than 5% were not included in the figures to easily identify trends among the major constituents. The following figures identify the main elements found on the Face and Cross samples for all steel pipes and for all copper pipes,. Analyses by location (MA, RI, and MD) is also included. For placing the sample on the microscope stage, copper tape was used to ground the sample and carbon tape was used to hold the sample in place for analyses, and could have impacted the weight percentages.

3.5.1 Steel Corrosion EDS Data

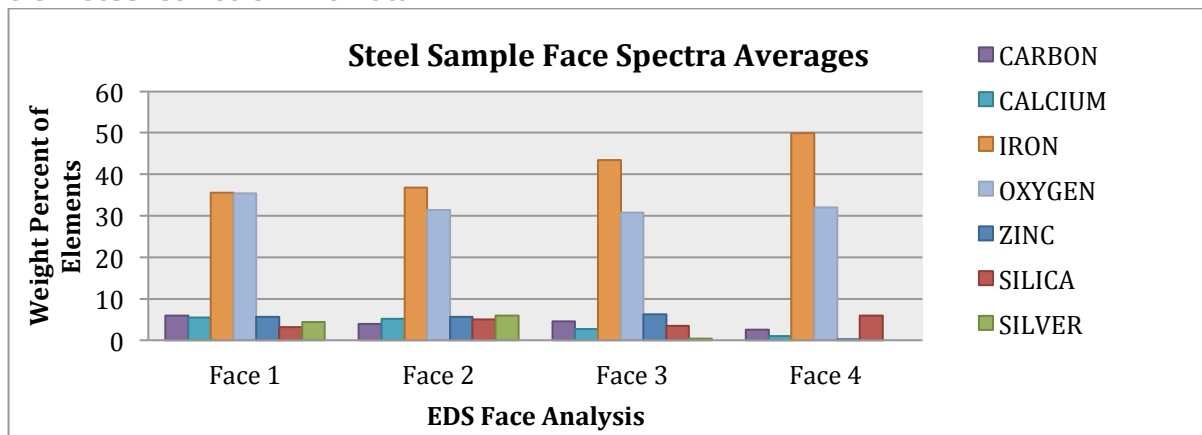


Figure 3: Steel Sample Elemental Face Composition

The averages calculated in Figure 3 for each of the Face values is for all steel samples from all three locations. The figure shows an overall decrease in elemental concentrations farther into the pipe for carbon, calcium, zinc, silica, and silver. The predominant elements from Face spectra are iron and oxygen, with iron concentrations increasing from 35% in Face 1 to 50% weight in Face 4.

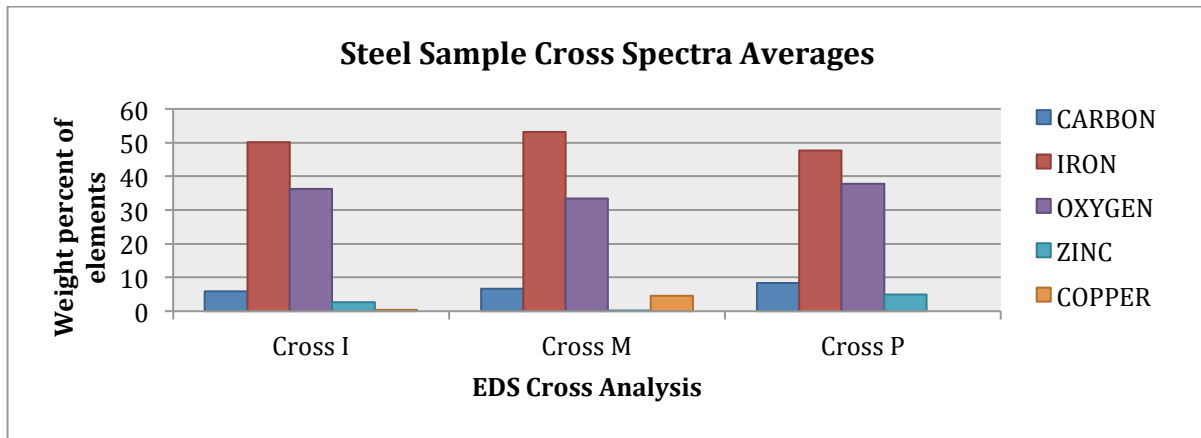


Figure 4: Steel Sample Elemental Cross-Section Composition

The predominant elements shown in Figure 4 for the steel Cross samples are iron and oxygen. The copper and zinc showed a reduction closer to pipe interior in comparison to the water interface. Carbon, zinc, and copper were all less than 10% in all samples. Iron comprised approximately 50% of the weight percent, and oxygen approximately 35%. There was not a discernable pattern in changes in composition with location.

3.5.2 Copper Corrosion EDS Data

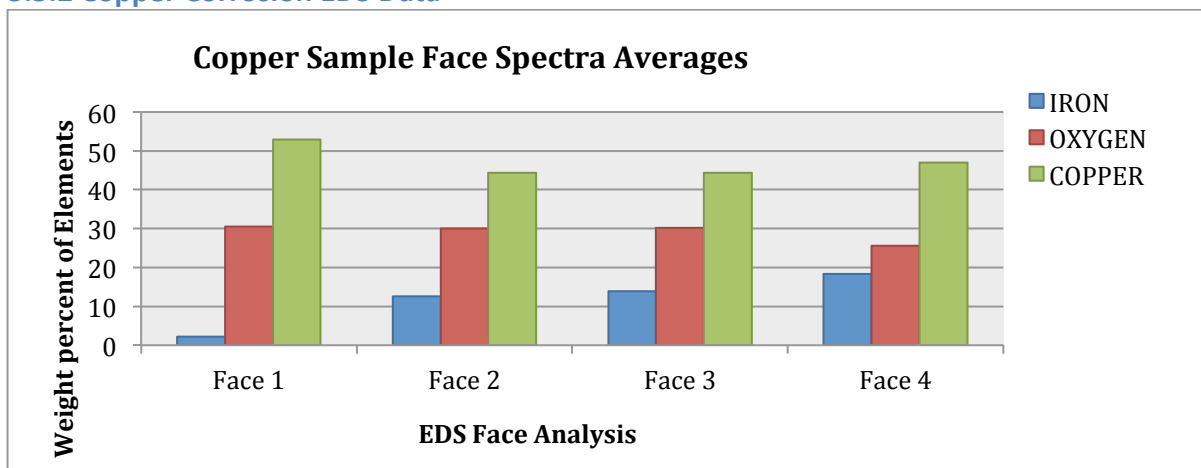


Figure 5: Copper Sample Elemental Face Composition

The predominant elements shown in Figure 5 for the copper Face samples are iron, oxygen, and copper. The oxygen concentration remained relatively constant at about 30% for all sample

points, while the copper showed minor variations between 44 and 52%. The high copper concentration can be a result of the pipe material itself. The iron concentration increased closer to the pipe interior than the water interface, starting at 2% for Face 1 samples, increasing to 18% for Face 4 samples.

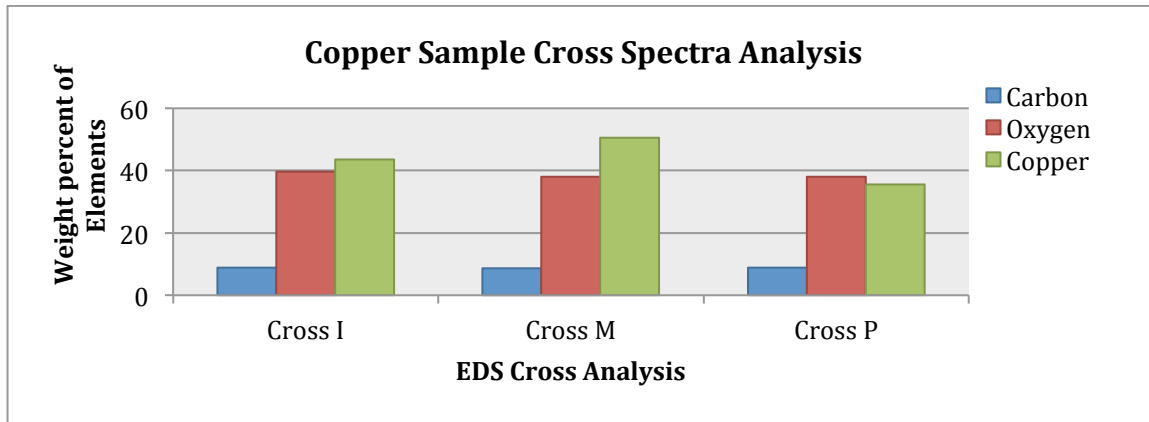


Figure 6: Copper Sample Elemental Cross-Section Composition

The predominant elements in Figure 6 for the copper Cross values are carbon, oxygen, and copper. Compared to the Face analysis, iron is not present and instead carbon is present. The oxygen concentration remained relatively constant at 40% by weight and the copper values had small fluctuations in weight percentages, between 35 and 50%. Carbon was below 10% in all samples.

3.5.3 MA Corrosion EDS Data

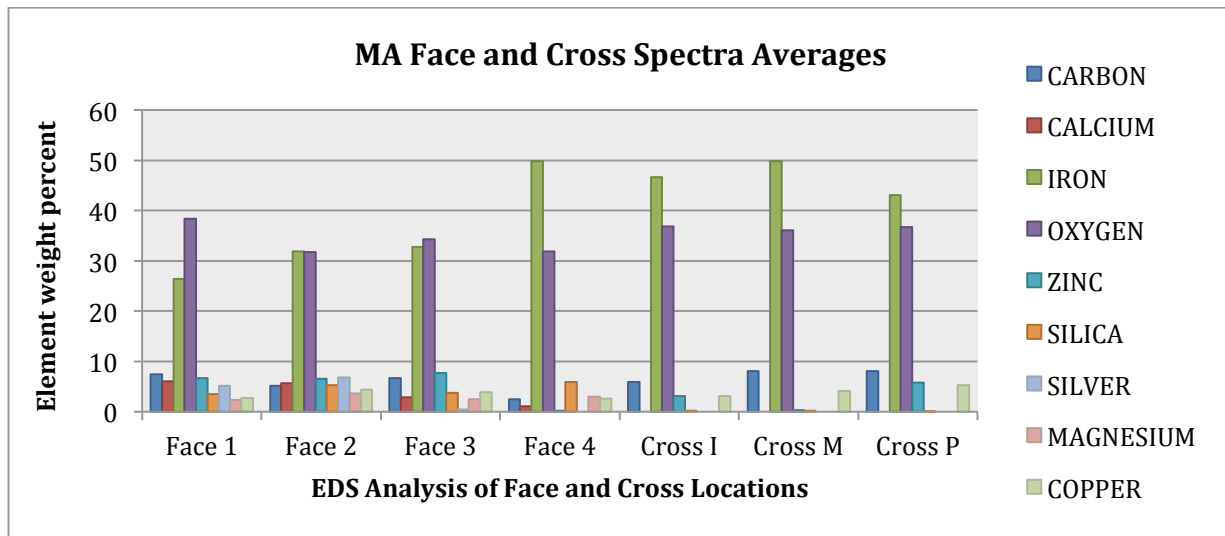


Figure 7: MA Face and Cross Elemental Composition

The predominant elements in Figure 7 for the MA pipe samples consisted of iron and oxygen. For the Face samples, the combined weight percent of iron and oxygen increased as the sample points became closer to the pipe interior while the other elements correspondingly decreased. The Cross values showed that iron and oxygen were similar across all the spectra points, while the other elements had small fluctuations or were not present.

3.5.4 RI Corrosion EDS Data

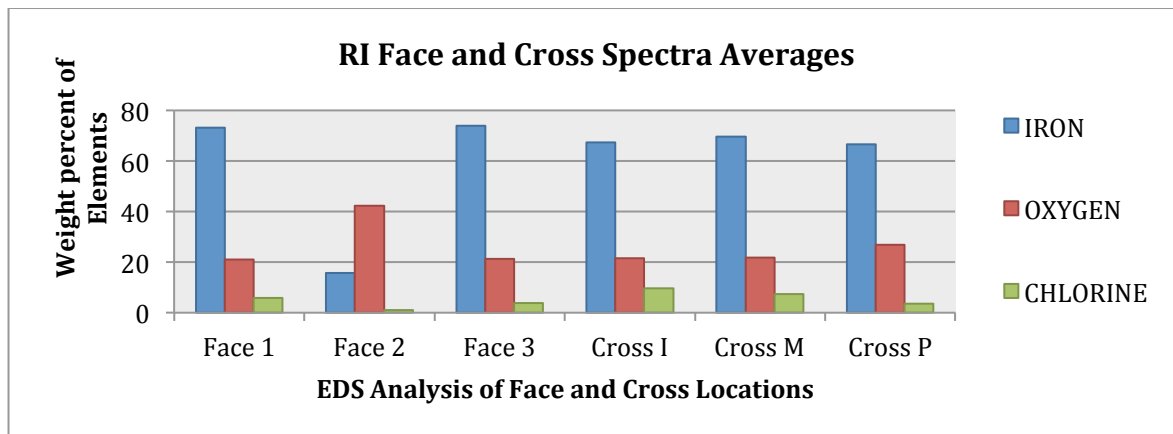


Figure 8: RI Face and Cross Elemental Composition

The predominant elements in Figure 8 for the RI Face and Cross samples included iron, oxygen, and chlorine. For RI, there was only one pipe sample made of galvanized steel. The element that had relatively constant concentrations was iron (67 to 73% for all locations except Face 2), with oxygen having some fluctuation from the different spectra points (21 to 42%). In comparison to iron, the chlorine values had smaller concentrations less than 10%.

3.5.5 MD Corrosion EDS Data

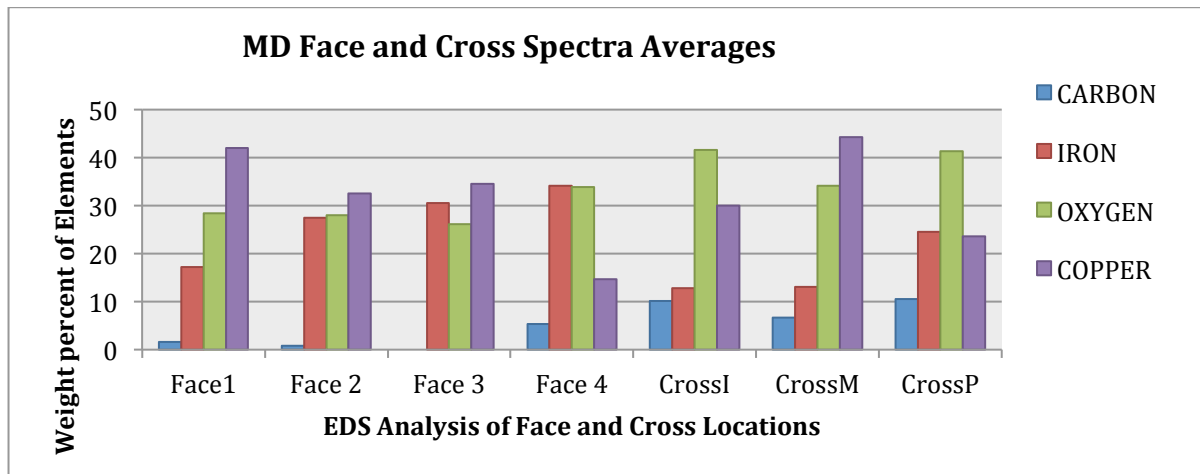


Figure 9: MD Face and Cross Elemental Composition

The predominant elements in Figure 9 for the MD Face and Cross samples included carbon, iron, oxygen, and copper. The carbon values were present at very low concentrations for the Face values (0.8 to 5%), and increased for the Cross spectra points (6 to 10%). The copper, iron, and oxygen concentrations were present at all sample points within the MD analysis.

3.6 Correlations between Water Quality and EDS Data

The following section correlates the elemental values from the EDS analysis to the water quality from the municipalities using the Pearson product-moment correlation coefficient as the statistical analysis. The correlations were done for steel face, steel cross, copper face, and copper

cross samples. The correlations could not be conducted for the individual municipalities because the water quality sample size was $N=1$.

Each Pearson value calculated is between -1, and +1, with the negative value showing an inverse correlation, zero showing no correlation, and the positive value as a direct correlation. Each parameter when correlated with itself has a value of 1.00. The calculated Pearson values are compared to tabulated critical values at a 95% confidence level ($\alpha = .05$) based on the number of data points (N). The critical values are readily available in published statistical references. Calculated absolute value correlations that are greater than the critical value indicate that the two parameters are correlated. The inversely correlated values are highlighted in yellow, and the directly correlated values are highlighted in green. The highlighting method is used for all of the steel and copper samples, but each sample set had different critical values and are specified below each table. The strength of the each correlation that is found to be statistically significant can be assessed based on Table 12 (Stats Tutor 2016).

Table 12: Strength of Correlation Value (Stats Tutor 2016)

Strength of Correlation	Range
Very Weak	0.0 – 0.19
Weak	0.2 – 0.39
Moderate	0.4 – 0.59
Strong	0.6 – 0.79
Very Strong	0.8 – 1.0

3.6.1 Steel Samples

Tables 13 and 14 show the correlations between the water quality and the steel face and steel cross EDS analysis. The respective critical value is below each sample and the strength analysis

of each correlation. In Table 13, the elements from the EDS analyses are listed first (including calcium), followed by the water quality parameters (including Ca). In the text “elemental” calcium refers to the elemental EDS analysis while “calcium” to the soluble concentration as provided in the municipal data reports.

Table 13: Steel EDS 'Face' Correlation with Water Quality

	Carbon	Calcium	Iron	Oxygen	Zinc	Silica	Silver	pH	Ca	Alk	TDS	Chloride	Sulfate
Carbon	1.00												
Calcium	0.76	1.00											
Iron	-0.80	-1.00	1.00										
Oxygen	0.65	0.54	-0.50	1.00									
Zinc	0.79	0.72	-0.79	0.08	1.00								
Silica	-0.94	-0.53	0.59	-0.47	-0.79	1.00							
Silver	0.47	0.93	-0.90	0.39	0.52	-0.18	1.00						
pH	1.00	0.31	-0.33	0.90	-0.23	-0.86	-0.07	1.00					
Ca	0.36	-0.77	0.75	-0.07	0.82	-0.79	-0.95	0.37	1.00				
Alkalinity	0.17	-0.88	0.87	-0.27	0.92	-0.66	-0.99	0.18	0.98	1.00			
TDS	0.96	0.03	-0.06	0.74	0.05	-0.97	-0.34	0.96	0.61	0.45	1.00		
Chloride	1.00	0.38	-0.40	0.93	-0.30	-0.82	0.01	1.00	0.30	0.10	0.94	1.00	
Sulfate	0.44	-0.71	0.70	0.01	0.77	-0.84	-0.92	0.45	1.00	0.96	0.68	0.38	1.00

The Steel Face data have a total sample set of $N = 47$, and the respective critical value is 0.2876. The carbon shared a weak direct correlation with the calcium, a moderate direct correlation with sulfate, and a very strong direct correlation with the pH, TDS, and chloride. The elemental calcium had a weak direct correlation with pH and chloride, a strong inverse correlation with calcium and sulfate, and a very strong inverse correlation with the alkalinity. The iron had a strong direct correlation with calcium and sulfate, a very strong correlation with the alkalinity, and a weak to moderate inverse correlation with the pH and chloride respectively. The oxygen had a strong direct correlation with the TDS, and a very strong direct correlation with the pH and

chlorides. The silica had a strong to very strong inverse correlation with every water quality parameter. Silver had a weak inverse correlation with the TDS and a very strong inverse correlation with the calcium, alkalinity, and sulfates.

Table 14: Steel EDS 'Cross' Correlation with Water Quality

	Carbon	Iron	Oxygen	Zinc	Copper	pH	Ca	Alk	TDS	Chloride	Sulfate
Carbon	1.00										
Iron	-0.64	1.00									
Oxygen	0.57	-1.00	1.00								
Zinc	0.67	-1.00	0.99	1.00							
Copper	-0.30	0.92	-0.96	-0.91	1.00						
pH	-0.47	-0.38	0.46	0.34	-0.70	1.00					
Ca	0.65	-1.00	0.99	1.00	-0.92	0.37	1.00				
Alkalinity	0.78	-0.98	0.96	0.99	-0.83	0.18	0.98	1.00			
TDS	-0.21	-0.62	0.69	0.59	-0.87	0.96	0.61	0.45	1.00		
Chloride	-0.54	-0.30	0.39	0.27	-0.65	1.00	0.30	0.10	0.94	1.00	
Sulfate	0.58	-1.00	1.00	0.99	-0.95	0.45	1.00	0.96	0.68	0.38	1.00

The total sample size for the steel cross samples is N = 41 with a critical value of 0.3081. The carbon had a moderate direct correlation with the sulfate, a strong direct correlation with the calcium and alkalinity, and a moderate inverse correlation with the pH and chloride. The iron had a weak inverse correlation with pH, a strong inverse correlation with TDS, and a very strong inverse correlation with calcium, alkalinity, and sulfate. The oxygen had a weak direct correlation with chloride, a moderate direct correlation with pH, and a very strong direct correlation with calcium, alkalinity, and sulfate. Zinc had a weak direct correlation with pH, a moderate direct correlation with TDS, and a very strong direct correlation with calcium, alkalinity, and sulfate. The copper had a strong inverse correlation with the pH and chloride, and a very strong inverse correlation with the calcium, alkalinity, TDS, and sulfates.

3.6.2 Copper Samples

Tables 15 and 16 identify the correlations between the water quality and copper samples. The same methodology used for the steel samples of identifying inverse and direct correlations is applied. The respective critical value is below each sample as well as strength analysis of each correlation.

Table 15: Copper EDS 'Face' Correlation with Water Quality

	Iron	Oxygen	Copper	pH	Ca	Alk	TDS	Chloride	Sulfate
Iron	1.00								
Oxygen	-0.71	1.00							
Copper	-0.79	0.13	1.00						
pH	-0.91	1.00	0.95	1.00					
Ca	0.05	0.31	0.05	0.37	1.00				
Alkalinity	0.25	0.12	-0.15	0.18	0.98	1.00			
TDS	-0.76	0.94	0.82	0.96	0.61	0.45	1.00		
Chloride	-0.94	1.00	0.97	1.00	0.30	0.10	0.94	1.00	
Sulfate	-0.03	0.39	0.13	0.45	1.00	0.96	0.68	0.38	1.00

The total sample size for the copper face samples is N = 22 with a critical value of 0.4227. The iron had a strong inverse correlation with the TDS, and a very strong inverse correlation with the pH and chloride. Oxygen had a very strong direct correlation with the pH, TDS, and chloride. The copper had a very strong direct correlation with pH, TDS, and chloride.

Table 16: Copper EDS 'Cross' Correlation with Water Quality

	Carbon	Oxygen	Copper	pH	Ca	Alkalinity	TDS	Chloride	Sulfate
Carbon	1.00								
Oxygen	-0.41	1.00							
Copper	-0.95	0.09	1.00						
pH	-0.05	0.93	-0.27	1.00					
Ca	0.91	0.01	-0.99	0.37	1.00				
Alkalinity	0.97	-0.18	-1.00	0.18	0.98	1.00			
TDS	0.23	0.80	-0.53	0.96	0.61	0.45	1.00		
Chloride	-0.13	0.96	-0.20	1.00	0.30	0.10	0.94	1.00	
Sulfate	0.87	0.10	-0.98	0.45	1.00	0.96	0.68	0.38	1.00

The total sample size for the copper face samples is N = 15 with a critical values of 0.5140. The carbon had a very strong direct correlation with calcium, alkalinity, and sulfate. The oxygen had a very strong direct correlation with pH, TDS, and chloride. The copper had a moderate inverse correlation with TDS, and a very strong inverse correlation with calcium, alkalinity, and sulfate.

3.7 Correlations between Corrosion Indices and EDS Data

Similarly to the water quality and EDS data comparison, this analysis correlates the LSI and Larson-Skold (LSK) values with respect to the EDS data. For the steel and copper pipe data, the LSIA and LSIB values for all three temperatures were used in addition to the three Larson-Skold values for each location. The critical value and strength of correlation is evaluated for the following data sets.

3.7.1 Steel Samples

Table 17 and 18 show the correlations for the steel samples with respect to the LSI and LSK values.

Table 17: Steel EDS 'Face' Correlation with LSI and LSK

	Carbon	Calcium	Iron	Oxygen	Zinc	Silica	Silver	LS1A-50	LSIA-110	LSIA-130	LS2B-50	LS2B-110	LS2B-130	LSK
Carbon	1.00													
Calcium	0.76	1.00												
Iron	-0.80	-1.00	1.00											
Oxygen	0.65	0.54	-0.50	1.00										
Zinc	0.79	0.72	-0.79	0.08	1.00									
Silica	-0.94	-0.53	0.59	-0.47	-0.79	1.00								
Silver	0.47	0.93	-0.90	0.39	0.52	-0.18	1.00							
LS1A-50	0.94	-0.01	-0.01	0.71	0.09	-0.98	-0.38	1.00						
LSIA-110	0.94	-0.01	-0.01	0.71	0.09	-0.98	-0.38	1.00	1.00					
LSIA-130	0.95	0.00	-0.03	0.72	0.08	-0.98	-0.37	1.00	1.00	1.00				
LS2B-50	0.91	-0.10	0.08	0.65	0.18	-0.99	-0.47	1.00	1.00	0.99	1.00			
LS2B-110	0.91	-0.10	0.08	0.65	0.18	-0.99	-0.47	1.00	1.00	0.99	1.00	1.00		
LS2B-130	0.92	-0.08	0.06	0.66	0.17	-0.99	-0.45	1.00	1.00	1.00	1.00	1.00	1.00	
LSK	0.96	0.58	-0.60	0.99	-0.51	-0.67	0.23	0.81	0.81	0.82	0.75	0.75	0.77	1.00

The Steel Face data has a total sample set of N = 47, and the respective critical value is 0.2876. Carbon had a very strong direct correlation with all the LSI values and LSK value. The calcium had a moderate direct correlation and iron had a strong inverse correlation with the LSK, but neither was correlated to the LSI values. The oxygen had a strong direct correlation with the LSI values and had a very strong direct correlation with the LSK. Zinc had a moderate inverse correlation with the LSK value. The silica had a very strong inverse correlation with the LSI values and a strong inverse correlation with the LSK value. The silver had a weak inverse correlation with LSIA and a moderate inverse correlation with LSIB, but was not correlation to the LSK.

Table 18: Steel EDS 'Cross' Correlation with LSI and LSK

	Carbon	Iron	Oxygen	Zinc	Copper	LS1A-50	LSIA-110	LSIA-130	LS2B-50	LS2B-110	LS2B-130	LSK
Carbon	1.00											
Iron	-0.64	1.00										
Oxygen	0.57	-1.00	1.00									
Zinc	0.67	-1.00	0.99	1.00								
Copper	-0.30	0.92	-0.96	-0.91	1.00							
LS1A-50	-0.16	-0.65	0.72	0.62	-0.89	1.00						
LSIA-110	-0.16	-0.65	0.72	0.62	-0.89	1.00	1.00					
LSIA-130	-0.17	-0.65	0.71	0.62	-0.89	1.00	1.00	1.00				
LS2B-50	-0.07	-0.72	0.78	0.69	-0.93	1.00	1.00	0.99	1.00			
LS2B-110	-0.07	-0.72	0.78	0.69	-0.93	1.00	1.00	0.99	1.00	1.00		
LS2B-130	-0.09	-0.71	0.77	0.68	-0.92	1.00	1.00	1.00	1.00	1.00	1.00	
LSK	-0.71	-0.09	0.18	0.05	-0.46	0.81	0.81	0.82	0.75	0.75	0.77	1.00

The total sample size for the steel cross samples is $N = 41$ with a critical value of 0.3081. The carbon had a strong inverse correlation with the LSK value. Iron had strong inverse correlations with the LSI values, while the oxygen and zinc had a strong direct correlation with the LSI values. The copper had a moderate inverse correlation with the LSK values and a very strong inverse correlation with the LSI values.

3.7.2 Copper Samples

Table 19 and 20 show the correlations for the copper samples with respect to the LSI and LSK values.

Table 19: Copper EDS 'Face' Correlation with LSI and LSK

	Iron	Oxygen	Copper	LS1A-50	LSIA-110	LSIA-130	LS2B-50	LS2B-110	LS2B-130	LSK
Iron	1.00									
Oxygen	-0.71	1.00								
Copper	-0.79	0.13	1.00							
LS1A-50	-0.73	0.92	0.79	1.00						
LSIA-110	-0.73	0.92	0.79	1.00	1.00					
LSIA-130	-0.73	0.93	0.80	1.00	1.00	1.00				
LS2B-50	-0.66	0.89	0.73	1.00	1.00	0.99	1.00			
LS2B-110	-0.66	0.89	0.73	1.00	1.00	0.99	1.00	1.00		
LS2B-130	-0.67	0.89	0.74	1.00	1.00	1.00	1.00	1.00	1.00	
LSK	-0.99	0.97	1.00	0.81	0.81	0.82	0.75	0.75	0.77	1.00

The total sample size for the copper face samples is $N = 22$ with a critical value of 0.4227. All three elements were correlated with all corrosion indices. The iron had a strong inverse correlation with the LSI values and a very strong inverse correlation with the LSK value. The oxygen had a very strong direct correlation with both the LSI and LSK values. The copper had a strong direct correlation with LSI A at 50°F and 110°F and all of the LSIB values. It also had a very strong direct correlation with the LSK values.

Table 20: Copper EDS 'Cross' Correlation with LSI and LSK

	Carbon	Oxygen	Copper	LS1A-50	LSIA-110	LSIA-130	LS2B-50	LS2B-110	LS2B-130	LSK
Carbon	1.00									
Oxygen	-0.41	1.00								
Copper	-0.95	0.09	1.00							
LS1A-50	0.27	0.77	-0.57	1.00						
LSIA-110	0.27	0.77	-0.57	1.00	1.00					
LSIA-130	0.26	0.78	-0.56	1.00	1.00	1.00				
LS2B-50	0.36	0.71	-0.64	1.00	1.00	0.99	1.00			
LS2B-110	0.36	0.71	-0.64	1.00	1.00	0.99	1.00	1.00		
LS2B-130	0.34	0.72	-0.63	1.00	1.00	1.00	1.00	1.00	1.00	
LSK	-0.34	1.00	0.02	0.81	0.81	0.82	0.75	0.75	0.77	1.00

The total sample size for the copper face samples is N = 15 with a critical values of 0.5140.

Carbon was not correlated with corrosion indices. The oxygen has a strong direct correlation with the LSI values and a very strong direct correlation with the LSK value. The copper has a moderate inverse correlation with the LSIA value and a strong inverse correlation with the LSIB values.

3.8 Summary of Correlations

Table 21 summarizes the respective elements found and the direct and inverse correlations to the water quality parameters and corrosion indices.

Table 21: Steel and Copper Correlation Comparison

Element	Steel				Copper			
	Face		Cross		Face		Cross	
	Direct Correlation	Inverse Correlation	Direct Correlation	Inverse Correlation	Direct Correlation	Inverse Correlation	Direct Correlation	Inverse Correlation
Carbon	pH, Calcium, TDS, Chloride, Sulfate, LSIA, LSIB, LSK		Calcium, Alkalinity, Sulfate	pH, Chloride, LSK			Calcium, Alkalinity, Sulfate	
Elemental Calcium	pH, Chloride, LSK	Calcium, Alkalinity, Sulfate			Not Present			
Copper				pH, Calcium, Alkalinity, TDS, Chloride, Sulfate, LSIA, LSIB, LSK	pH, TDS, Chloride, LSIA, LSIB, LSK			Calcium, Alkalinity, TDS, Sulfate, LSIA, LSIB,
Iron	Calcium, Alkalinity, Sulfate	pH, Chloride, LSK		pH, Calcium, Alkalinity, TDS, Sulfate, LSIA, LSIB		pH, TDS, Chloride, LSIA, LSIB, LSK		
Oxygen	pH, TDS, Chloride, LSIA, LSIB, LSK		pH, Calcium, Alkalinity, TDS, Chloride, Sulfate	LSIA, LSIB	pH, TDS, Chloride, LSIA, LSIB, LSK		pH, TDS, Chloride, LSIA, LSIB, LSK	
Silica		pH, Calcium, Alkalinity, TDS, Chloride, Sulfate, LSIA, LSIB, LSK			Not Present			
Silver		Calcium, Alkalinity, TDS, Sulfate, LSIA, LSIB			Not Present			
Zinc	Calcium, Alkalinity	LSK		pH, Calcium, Alkalinity, TDS, Sulfate	Not Present			

4.0 Discussion

Analyzing the summary correlation table yielded certain trends among the water quality parameters in addition to the index values with respect to the EDS data. To get a holistic representation of what is occurring in the system Table 21 shown previously juxtaposes the EDS data with the water quality parameters that influence the rate of corrosion and the LSIA, LSIB, LSK values that can determine the propensity for corrosion.

4.1 Analysis of Results

The following sections analyze the correlations between the water quality, LSI and Larson Skold values, and the EDS data for the steel and copper piping.

4.1.1 Steel and Copper Analysis

The steel and copper Face and Cross analyses were a comprehensive review of overall changes that were occurring in the distribution system. Table 21 incorporates water quality from three different locations to identify relationships and the correlations. Due to the water quality data limitations for the individual locations, the systems' propensity to experience corrosion was analyzed based on the elemental correlations with the water quality and indices based on pipe material.

4.1.1.1 Steel

The elements found within the steel samples showed some variation between correlations for the face and cross spectra samples. The carbon shared direct correlations with the face and cross values for the calcium and sulfate parameters. Iron showed an inverse correlation for both face and cross for the pH in comparison to oxygen that showed a direct correlation between the pH, TDS, and chloride parameters. The other elements shared an inverse correlation with many water quality parameters with only particular data sets or did not have any common parameters from different sample locations.

4.1.1.2 Copper

The copper sample set had few elements present resulting in minimal comparison between the face and cross values. The only element that had direct correlations for both face and cross samples was oxygen. Oxygen had a direct correlation for the pH, TDS, chloride, LSIA, LSIB, and LSK for face and cross samples. The iron had an inverse correlation to the parameters oxygen shared a direct correlation with, showing that as the oxygen concentration increased, the iron concentration decreased and vice versa.

4.1.2 MA Analysis

The primary pipe material for MA consisted of steel for the distribution system. Based on the correlations for the steel, an increase in the calcium and sulfate concentrations will increase carbon concentration in interior pipe deposits. An increase in pH, TDS, and chloride concentration will be directly linked to oxygen concentrations in pipe deposits. The iron concentration is inversely linked to the pH value of the system. Based on the propensity of corrosion product of the steel this can be compared to the source water of the MA municipality.

The elevated chlorides in the MA water supply could result from chlorides or chemicals added during treatment. There are the two chlorination processes, the first chlorination process is before the water reaches the storage tanks, and the second process is a chloramine dose before distribution to ensure residual chlorine. However, doses in the mg/L range would only add small concentration of chlorides to the water. To find the source of the elevated chlorides, monitoring in the watershed for point and non-point sources could be conducted.

As discussed earlier, the two mechanisms analyzed by the Technical Institute in Lisbon, Portugal identified the formation of ferric oxides and ferric chlorides as a result of chloride displacing the oxygen (Montemor 2003). Considering the oxygen concentration shares a direct correlation with the chloride concentration this mechanism could occur in the system. In

contrast, the elevated chlorides can react with the inner diameter of the pipe creating different methods of corrosion to occur such as pitting and crevice corrosion that leads to pipe material leaching (Montemor 2003) which can be explained by the carbon from the carbon steel pipes.

4.1.3 RI Analysis

The material used for the RI well pipe was galvanized steel. Considering this pipe exhibited visible rust formations, an increase in oxygen in the system as a result of chloride could have contributed to the formation of ferric oxides. In addition to chloride, the steel pipes indicated that a decreased pH would increase iron weight percentages. Since the pH of this system was 6.6, this can correspond to the elevated iron in the water. If there are elevated levels of free iron in solution the growth of iron reducing bacteria (IRB) can occur (Kakooei et al. 2012, Montemor 2003).

4.1.4 MD Analysis

The primary materials for MD consisted of copper piping with two carbon steel pipes. The only element from the copper sample set that correlated to the pH, TDS, chloride, and corrosion indices was oxygen.

The use of orthophosphate in the treatment plant process can explain the relationship between the oxygen with the water chemistry. The chloride levels for MD water quality were not elevated, but there was observable deposition on the pipe interior. A study by Zhang et al. (2012) analyzed copper coupons with 0.5 mg/L and 1 mg/L concentrations for both orthophosphate and polyphosphate with residual chlorine in the system. The copper samples with the inhibitor reduced the free chlorine degradation by either forming a protective layer on the metal or by reducing the concentration of copper ions (Zhang et al. 2012). The natural reactivity of the copper in conjunction with the water chemistry can contribute to the oxygen deposition on the pipe as a protective passive layer; however, if the oxygen concentration decreased in addition to

a negative LSIA, LSIB, and LSK, the iron concentration would increase suggesting the formation of iron reducing bacteria (Kakooei et al. 2012).

4.2 Alternative Corrosion Control Methods

Current techniques to prevent degradation of the distribution system include adjusting the pH adding corrosion control chemicals to decrease the corrosion potential are (Singeley 1984).

Chemicals include zinc-orthophosphate, poly-orthophosphate (Cohen 2003), polyphosphate, and lime. Alternatives to the phosphate-based inhibitors include the use of special coatings for pipes and sodium silicate.

4.2.1 Interior Pipe Coatings

A way to prevent scale formation and corrosion of piping systems is the use of engineered coatings on the interior of the pipe. Although this is practical, it can only be done if a new piping system is implemented. The coatings can be effective but can create a high friction boundary in the pipe, which can be detrimental if there are high amounts of total dissolved solids. The prevalent coatings include coal tar enamel, epoxy, cement mortar, and polyethylene (Singeley 1984). Table 22 below identifies the advantages and disadvantages for each proposed lining.

Table 22: Coatings for Pipe Walls (Singeley 1984)

Material	Application	Advantages	Disadvantages
Hot Coal Tar Enamel	Steel Pipes in distribution systems	Service life over 50 years, Corrosion resistance to high TDS and biofilm formation	Needs reapplication to welded areas, extreme heat can cause stress corrosion, and extreme cold can cause brittleness, elevated trace organics
Epoxy	Steel and ductile iron pipes	Smooth finish decreases head loss in pipes, approved by the Food and Drug Administration (FDA)	Expensive, less resistant than coal tar, service life less than 15 years
Cement Mortar	Ductile iron pipes, sometimes steel or cast-iron	Inexpensive, can be applied in a system already built, calcium hydroxide release provides protective scale for pipe joints	Coating rigidity and lead to cracking and stress corrosion, thickness of coating increases head loss and decreases flow capacity
Polyethylene	Ductile Iron and steel	Service life over 50 years, Corrosion resistance to high TDS and biofilm formation, and decreased head loss due to finish	Expensive Process

A major factor that influences a coating selection is the direct affect to public health and the source water quality. For potable systems compliance with federal drinking water standards would be necessary. For HVAC systems, a broader array of alternatives can be considered.

4.2.2 Sodium Silicate

The use of sodium silicate has been used to reduce the corrosivity of the water for over fifty years in distribution systems. This compound forms a protective layer on the interior diameter of the pipe and reduces the corrosion of galvanized iron, brass, and copper plumbing systems (Singeley 1984). The effectiveness is dependent on the pH and the bicarbonate concentration with the source water. The ideal feed rate of this inhibitor is 2 to 8 mg/L with a maximum dose of 12 mg/L to create the protective film (Singeley 1984). The ideal implementation of this method would be for water with pH 8, very low hardness and alkalinity, under high velocity flow conditions.

4.3 Recommendations

The MA and RI treatment plants used pH adjustment for corrosion control; however, pH adjustment alone may not be insufficient to control corrosion in waters that have low carbonate and bicarbonate (Singeley 1984). For municipalities that do not have CaCO_3 , deposition raising the pH above 8 is necessary. EPA regulations suggest the use of lime, caustic soda, soda ash, and sodium bicarbonate for pH adjustment (Singeley 1984), and both the MD and RI treatment facilities utilized lime for pH adjustment. With the elevated chloride levels in the MA distribution system, a different inhibitor could be used to reduce the reactivity of chlorine and chloride in the system. The RI facility could consider raising the pH from 6.6 to above 8 (Singeley 1984) prior to distribution. The low pH of the water from distribution can be responsible for creating aggressive water causing corrosion. In addition to pH control, a corrosion inhibitor can be implemented based on the LSK value. The treatment plant for MD

uses lime and orthophosphate to reduce corrosion in their system, but some corrosion occurred in the tested pipe samples despite the corrosion control. An increase in the orthophosphate dose could potentially reduce the corrosion, considering the LSK value indicated corrosion would occur based on the finished water quality at the treatment plant. An important factor to consider when analyzing the specific locations is potential changes in the water chemistry based on chemical additions at the apartment complexes; thus the characteristics of the water in the pipe samples may differ from the characteristics provided by the municipality water quality reports.

4.4 Future Research into Phosphate Mechanisms

The current phosphate blends that are available for corrosion control include: zinc-orthophosphate, poly-orthophosphate (Cohen 2003), polyphosphate, glassy phosphates such as sodium hexametaphosphate (Singeley 1984, Ripp 2000), and bimetallic polyphosphates. The exact science behind the corrosion control chemistry between phosphates and the water chemistry requires lab and field tests based on flow rate, concentration of inhibitor, pH, temperature, calcium, and carbonate levels in order to choose the right phosphate blend. The phosphate can coat the interior surfaces of the piping that can slow down the rate of corrosion occurring. EPA regulations recommend low doses of glassy phosphates with concentrations between 2 to 4 mg/L for controlling iron release. Control of metal loss requires significantly higher doses, on the order of 20 to 40 mg/L (Singeley 1984).

4.4.1 Application of Phosphate: Experimental Tests

A bench scale pilot study by Abernathy (2006) utilized different types of phosphate inhibitors to prevent corrosion of the piping system with different disinfectant residuals. The bench scale studies utilized reactors that replicated systems with residual concentrations of chlorine and mono-chloramines in the range of 0.15 mg/L to 0.25 mg/L. The metals tested included mild steel and iron samples to simulate pipe material in order to test the efficacy of

zinc-orthophosphate and polyphosphate as corrosion inhibitors. The recommended phosphate dose of 5 mg/L was the optimal dose to reduce the reactivity of residual chlorine (Abernathy 2006).

The use of the corrosion inhibitors are effective but has slow reaction kinetics requiring long contact times. The phosphate additionally reduces the disinfection efficiency of secondary disinfectants (Abernathy 2006). The study concluded that the optimal dose of polyphosphate for free chlorine residual was 8 mg/L to mitigate the reactivity of the chlorine with cations in solution, causing the chlorine to react more efficiently with biofilms. The recommended dose from this study is also the dose suggested per EPA standards (Singeley 1984). The formation of corrosion products in the presence of the inhibitor proved to be less reactive enabling the monochloramine to inactivate the microbes and control biofilms more efficiently than without an inhibitor.

4.5 Limitations of Analysis

Some of factors that can affect the overall assumptions and correlations made in this report are the water quality data of the treated water after it leaves the treatment plant with respect to the water received at the tap. All of the water quality information used for this study consisted of water quality reports of finished water at the treatment plant. Considering reactions that occur in the distribution system and chemicals that can be added at an apartment complex, water quality in the apartment buildings can show different correlations between elemental constituents and water quality parameters. Having additional data on corrosion control programs at point of use can provide information on efficacy of inhibitors for mitigating corrosion.

Although the SEM EDS data provides a clear representation of the elements in each sample, this analysis does not identify specific compounds formed. A study by Burleigh et al. (2014) utilized SEM with EDS as well as X-Ray Diffraction (XRD) for pitting corrosion in

copper pipes. XRD testing can be done with solid samples or powder samples and identifies the compounds formed within the sample and the respective phases of that compound. The benefit of doing an SEM analysis first yields the elements present, so the XRD analysis can search for those specific elements and the compounds that form as a result. This analysis could be helpful in identifying more correlations between the water quality parameters and the specific corrosion products that formed as a result.


References

- Abernathy, C. "Interactions between pipe materials, organics, corrosion inhibitors, and disinfectants on distribution biofilms" Volume 1 : Bench and Pilot-Scale Studies." Center for Biofilm Engineering, Montana State University, Bozeman, MT. *National Water Research Institute (2006)* 1 n. pag. Print.
- Rosemount Analytical. "Measuring Total Dissolved Solids (TDS) With a TDS Meter." *RSS. Emerson Process Management*, 22 Aug. 2012. Web.
- Beech, I., Bergel, A., Mollica, A. et al. "Simple Methods for the Investigation of of the Role of Biofilms in Corrosion SIMPLE METHODS FOR THE INVESTIGATION OF THE ROLE OF." *Biocorrosion Network* September (2000): 0–27. Print.
- Burleigh, T., Gierke, C., Fredj, N. et al. "Copper Tube Pitting in Santa Fe Municipal Water Caused by Microbial Induced Corrosion." *Materials* 7.6 (2014): 4321–4334. Web.
- Chang, T., and F. Lansing. "Review of Corrosion Causes and Corrosion Control in a Technical Facility." *DSN Engineering Section* (1982): n. pag. Print.
- Chawla, V, Gurbuxani, P.G., Bhagure, G. R. et al. "Corrosion of Water Pipes : A Comprehensive Study of Deposits." *Journal of Mineral & Materials Characterization & Engineering* 11.5 (2012): 479–492. Print.
- Cohen, Y., Koby, C.H. et al. "Corrosion Control Aids Residuals." *Journal of the American Water Works Association* (2003) 29.1 1–5. Web.
- Farida, W., Hemmingsen, T., Berntsen, T. et al. "Effect of Precorrosion and Temperature on the Formation Rate of Iron Carbonate Film." *7th Pipeline Technology Conference*, Estrel Convention Center, Berlin, Germany (2012): n. pag. Print.
- Geiger, G., and Esmacher, M. J. "Controlling Corrosion in Cooling Water Systems - Part 2: Inhibiting and Monitoring Corrosion." *Chemical Engineering Progress* 108.3 (2012): 29–34. Web.
- Gerhardus H. K., Michiel, P.H., and Thompson, N. G., Virmani, Y.P., Brongers, J.H. "Corrosion Costs and Preventive Strategies in the United States." *NACE International* (2002): 1–12. Web.
- Javaherdashti, R. "Microbiologically Influenced Corrosion (MIC)." *Microbiologically Influenced Corrosion. An Engineering Insight* MIC (2008): 29–71. Web.
- Kakooei, S., Ismail, M.C., Ariwahjoedi, B. "Mechanisms of Microbiologically Influenced Corrosion : A Review." *World Applied Sciences Journal* 17.4 (2012): 524–531. Print.



- Kim, D., Cha, J., Hong, S. et al. "Control of Corrosive Water in Advanced Water Treatment Plant by Manipulating Calcium Carbonate Precipitation Potential." *Korean Journal of Chemical Engineering* 26.1 (2009): 90–101. Web.
- Kritzer, P. "Corrosion in High-Temperature and Supercritical Water and Aqueous Solutions: A Review." *The Journal of Supercritical Fluids* 29.1-2 (2004): 1–29. Web.
- "Lead and Copper Rule." *EPA*. Environmental Protection Agency, 2004. Web. 28 Apr. 2016.
- Lahlou, M.Z. "Water Quality in Distribution Systems." *A National Drinking Water Clearinghouse Fact Sheet*, National Environmental Services Center (2003): 1. Print.
- LeChevallier, M.W., Lowry, C., Lee, R., Gibbon, D. et al. "Examining the Relationship between Iron Corrosion and the Disinfection of Biofilm Bacteria." *Journal of American Water Works Association*, 85.7 (2016): 111–123. Print.
- Leitz, F. and Guerra, K. "Water Chemistry Analysis for Water Conveyance, Storage, and Desalination Projects." *U.S. Department of the Interior, Bureau of Reclamation, Denver, CO*. August (2013): n. pag. Print.
- McDougall, J.L., L. McCall, and M.E. Stevenson. "Water Chemistry and Processing Effects on the Corrosion Degradation of Copper Tubing in Cooling Water Systems." *Practical Failure Analysis* 3. October (2003): 81–88. Web.
- Montemor, M. F., A. M P Simes, and M. G S Ferreira. "Chloride-Induced Corrosion on Reinforcing Steel: From the Fundamentals to the Monitoring Techniques." *Cement and Concrete Composites*. 25.4-5 SPEC (2003): 491–502. Web.
- Oliphant, R J. "Causes of Copper Corrosion in Plumbing Systems." *Foundation of Water Research* 44.0 (2010): 1–33. Print.
- Stats Tutor UK*. "Pearson's Correlation" Loughborough University, Coventry Universities, and Sigma network, statistical resource center. April 28, 2016. n. pag.
- Ripp, Kevin M. "Causes and Cures System Corrosion." *Journal of American Water Works Association*. 25 (2000): 26–28. Print.
- Singeley, J., Beaudet, B., Markey, P. "Corrosion Manual for Internal Corrosion of Water Distribution Systems." *EPA* 1984: 570/9-84-001. 1–142. Print.
- Wan, Y., Wang, X. Sun, H. et al. "Corrosion Behavior of Copper at Elevated Temperature." *International Journal of Electrochemical Science* 7 (2012): 7902–7914. Print.
- Zhang, H., and S. Andrews. "Effects of phosphate based corrosion inhibitors on the kinetics of chlorine degradation and halo acetic acid formation in contact with three metals." *Canadian Journal of Civil Engineering* 39.1. Jan 2012 (2012): 44. Web.





Appendices


Appendix A: Pipe Sample Information

#	Photograph	Characterization	
2		Material	Galvanized Steel
		Component	Pipe
		Diameter	4in
		System	Dry Sprinkler
		Temperature	Cold
		Loop	Open
3		Material	Galvanized Steel
		Component	Well Pipe
		Diameter	3in
		System	Potable
		Temperature	Cold
		Loop	Open
4		Material	Carbon Steel
		Component	Pipe
		Diameter	4in
		System	Wet Sprinkler
		Temperature	Cold
		Loop	Open
5		Material	Carbon Steel
		Component	Pipe
		Diameter	2in
		System	HVAC
		Temperature	Hot
		Loop	Closed
6		Material	Steel
		Component	Manifold Pipe
		Diameter	3in
		System	HVAC
		Temperature	Hot
		Loop	Closed

7			<table border="1"> <tr><td>Material</td><td>Copper</td></tr> <tr><td>Component</td><td>Pipe</td></tr> <tr><td>Diameter</td><td>2in</td></tr> <tr><td>System</td><td>Potable</td></tr> <tr><td>Temperature</td><td>Cold</td></tr> <tr><td>Loop</td><td>Open</td></tr> </table>	Material	Copper	Component	Pipe	Diameter	2in	System	Potable	Temperature	Cold	Loop	Open
Material	Copper														
Component	Pipe														
Diameter	2in														
System	Potable														
Temperature	Cold														
Loop	Open														
8			<table border="1"> <tr><td>Material</td><td>Carbon Steel</td></tr> <tr><td>Component</td><td>Spool</td></tr> <tr><td>Diameter</td><td>4in</td></tr> <tr><td>System</td><td>HVAC</td></tr> <tr><td>Temperature</td><td>Warm</td></tr> <tr><td>Loop</td><td>Closed Loop</td></tr> </table>	Material	Carbon Steel	Component	Spool	Diameter	4in	System	HVAC	Temperature	Warm	Loop	Closed Loop
Material	Carbon Steel														
Component	Spool														
Diameter	4in														
System	HVAC														
Temperature	Warm														
Loop	Closed Loop														
9			<table border="1"> <tr><td>Material</td><td>Carbon Steel</td></tr> <tr><td>Component</td><td>Spool</td></tr> <tr><td>Diameter</td><td>4in</td></tr> <tr><td>System</td><td>HVAC</td></tr> <tr><td>Temperature</td><td>Warm</td></tr> <tr><td>Loop</td><td>Closed Loop</td></tr> </table>	Material	Carbon Steel	Component	Spool	Diameter	4in	System	HVAC	Temperature	Warm	Loop	Closed Loop
Material	Carbon Steel														
Component	Spool														
Diameter	4in														
System	HVAC														
Temperature	Warm														
Loop	Closed Loop														
10.1			<table border="1"> <tr><td>Material</td><td>Copper</td></tr> <tr><td>Component</td><td>Pipe</td></tr> <tr><td>Diameter</td><td>2in</td></tr> <tr><td>System</td><td>Potable</td></tr> <tr><td>Temperature</td><td>Cold</td></tr> <tr><td>Loop</td><td>Open</td></tr> </table>	Material	Copper	Component	Pipe	Diameter	2in	System	Potable	Temperature	Cold	Loop	Open
Material	Copper														
Component	Pipe														
Diameter	2in														
System	Potable														
Temperature	Cold														
Loop	Open														
10.4			<table border="1"> <tr><td>Material</td><td>Copper</td></tr> <tr><td>Component</td><td>Pipe</td></tr> <tr><td>Diameter</td><td>1.5 in</td></tr> <tr><td>System</td><td>HVAC</td></tr> <tr><td>Temperature</td><td>Hot Water</td></tr> <tr><td>Loop</td><td>Closed</td></tr> </table>	Material	Copper	Component	Pipe	Diameter	1.5 in	System	HVAC	Temperature	Hot Water	Loop	Closed
Material	Copper														
Component	Pipe														
Diameter	1.5 in														
System	HVAC														
Temperature	Hot Water														
Loop	Closed														

10.5			<table border="1"> <tr><td>Material</td><td>Copper</td></tr> <tr><td>Component</td><td>Elbow fitting</td></tr> <tr><td>Diameter</td><td>.5 in</td></tr> <tr><td>System</td><td>HVAC</td></tr> <tr><td>Temperature</td><td>Hot</td></tr> <tr><td>Loop</td><td>Closed</td></tr> </table>	Material	Copper	Component	Elbow fitting	Diameter	.5 in	System	HVAC	Temperature	Hot	Loop	Closed	
Material	Copper															
Component	Elbow fitting															
Diameter	.5 in															
System	HVAC															
Temperature	Hot															
Loop	Closed															
10.6			<table border="1"> <tr><td>Material</td><td>Copper</td></tr> <tr><td>Component</td><td>Pipe</td></tr> <tr><td>Diameter</td><td>1in</td></tr> <tr><td>System</td><td>Potable</td></tr> <tr><td>Temperature</td><td>Cold</td></tr> <tr><td>Loop</td><td>Open</td></tr> </table>	Material	Copper	Component	Pipe	Diameter	1in	System	Potable	Temperature	Cold	Loop	Open	
Material	Copper															
Component	Pipe															
Diameter	1in															
System	Potable															
Temperature	Cold															
Loop	Open															
10.7			<table border="1"> <tr><td>Material</td><td>Copper</td></tr> <tr><td>Component</td><td>Pipe</td></tr> <tr><td>Diameter</td><td>1.25in</td></tr> <tr><td>System</td><td>Potable</td></tr> <tr><td>Temperature</td><td>Cold</td></tr> <tr><td>Loop</td><td>Open</td></tr> </table>	Material	Copper	Component	Pipe	Diameter	1.25in	System	Potable	Temperature	Cold	Loop	Open	
Material	Copper															
Component	Pipe															
Diameter	1.25in															
System	Potable															
Temperature	Cold															
Loop	Open															
10.8			<table border="1"> <tr><td>Material</td><td>Copper</td></tr> <tr><td>Component</td><td>Pipe</td></tr> <tr><td>Diameter</td><td>.75in</td></tr> <tr><td>System</td><td>Potable</td></tr> <tr><td>Temperature</td><td>Cold</td></tr> <tr><td>Loop</td><td>Open</td></tr> </table>	Material	Copper	Component	Pipe	Diameter	.75in	System	Potable	Temperature	Cold	Loop	Open	
Material	Copper															
Component	Pipe															
Diameter	.75in															
System	Potable															
Temperature	Cold															
Loop	Open															
11.1			<table border="1"> <tr><td>Material</td><td>Carbon Steel</td></tr> <tr><td>Component</td><td>Pipe</td></tr> <tr><td>Diameter</td><td>2in</td></tr> <tr><td>System</td><td>HVAC</td></tr> <tr><td>Temperature</td><td>Hot</td></tr> <tr><td>Loop</td><td>Open</td></tr> </table>	Material	Carbon Steel	Component	Pipe	Diameter	2in	System	HVAC	Temperature	Hot	Loop	Open	
Material	Carbon Steel															
Component	Pipe															
Diameter	2in															
System	HVAC															
Temperature	Hot															
Loop	Open															

11.2		<table border="1"> <tr><td>Material</td><td>Carbon Steel</td></tr> <tr><td>Component</td><td>Pipe</td></tr> <tr><td>Diameter</td><td>2in</td></tr> <tr><td>System</td><td>HVAC</td></tr> <tr><td>Temperature</td><td>Hot</td></tr> <tr><td>Loop</td><td>Open</td></tr> </table>	Material	Carbon Steel	Component	Pipe	Diameter	2in	System	HVAC	Temperature	Hot	Loop	Open	
Material	Carbon Steel														
Component	Pipe														
Diameter	2in														
System	HVAC														
Temperature	Hot														
Loop	Open														
11.4		<table border="1"> <tr><td>Material</td><td>Carbon Steel</td></tr> <tr><td>Component</td><td>Pipe</td></tr> <tr><td>Diameter</td><td>2.25in</td></tr> <tr><td>System</td><td>HVAC</td></tr> <tr><td>Temperature</td><td>Hot</td></tr> <tr><td>Loop</td><td>Open</td></tr> </table>	Material	Carbon Steel	Component	Pipe	Diameter	2.25in	System	HVAC	Temperature	Hot	Loop	Open	
Material	Carbon Steel														
Component	Pipe														
Diameter	2.25in														
System	HVAC														
Temperature	Hot														
Loop	Open														
11.5		<table border="1"> <tr><td>Material</td><td>Carbon Steel</td></tr> <tr><td>Component</td><td>Pipe</td></tr> <tr><td>Diameter</td><td>2in</td></tr> <tr><td>System</td><td>HVAC</td></tr> <tr><td>Temperature</td><td>Hot</td></tr> <tr><td>Loop</td><td>Open</td></tr> </table>	Material	Carbon Steel	Component	Pipe	Diameter	2in	System	HVAC	Temperature	Hot	Loop	Open	
Material	Carbon Steel														
Component	Pipe														
Diameter	2in														
System	HVAC														
Temperature	Hot														
Loop	Open														
11.8		<table border="1"> <tr><td>Material</td><td>Carbon Steel</td></tr> <tr><td>Component</td><td>Pipe</td></tr> <tr><td>Diameter</td><td>2.25in</td></tr> <tr><td>System</td><td>HVAC</td></tr> <tr><td>Temperature</td><td>Hot</td></tr> <tr><td>Loop</td><td>Open</td></tr> </table>	Material	Carbon Steel	Component	Pipe	Diameter	2.25in	System	HVAC	Temperature	Hot	Loop	Open	
Material	Carbon Steel														
Component	Pipe														
Diameter	2.25in														
System	HVAC														
Temperature	Hot														
Loop	Open														

12.1		Material	Copper/Brass
		Component	Valve
		Diameter	.75in
		System	Potable
		Temperature	Hot/Cold
		Loop	Open

Appendix B: SEM Sample Spectra Reports

In Attached Document: Example Below

Project 2

Spectrum processing :
No peaks omitted

Processing option : Oxygen by stoichiometry (Normalised)
Number of iterations = 2

Standard :

Fe Fe 1-Jun-1999 12:00 AM
Zn Zn 1-Jun-1999 12:00 AM

Element	Weight%	Atomic%	Compd%	Formula
Fe K	3.11	2.26	4.01	FeO
Zn K	77.12	47.74	95.99	ZnO
O	19.77	50.00		
Totals	100.00			

